

THE ACTIONS OF MOUSE MAST CELL PROTEASE-7
AND CALCIUM-ACTIVATED POTASSIUM CHANNEL
INHIBITORS ON PAR2-INDUCED RELAXATION OF THE
AORTA IN MICE

JAMES CHRISTOPHER KING



**The Actions of Mouse Mast Cell Protease-7 and Calcium-Activated Potassium
Channel Inhibitors on PAR2-Induced Relaxation of the Aorta in Mice**

By © James Christopher King

**Submitted to the School of Graduate Studies in partial fulfillment of the
requirements for the degree of Masters of Science (Medicine)**

Memorial University

February 2009

St. John's, Newfoundland & Labrador

Table of Contents

Abstract	i
Acknowledgements	ii
Co-Authorship	iii
List of Figures	iv
List of Abbreviations	vi
Introduction	1
Background	1
PAR2-Activating Peptides	2
PAR2-Dependent Relaxation of Vascular Smooth Muscle	5
Calcium-Activated Potassium Channels (K_{Ca})	7
Characteristics of Mast Cells	10
Tryptase	11
PAR2 and Human Mast Cell β -Tryptase Relationship	12
Glycosylation of PAR2	13
PAR2 and Inflammation	14
Rationale, Hypothesis, Objectives	15
Methods and Materials	17
Animals	17
Materials	17
Measurements of Isometric Tension in Aorta of Mice	17
Measurement of the Relative Serine Proteinase Activity of Purified mMCP-7, hMC β - Tryptase and Bovine Trypsin by Absorbance Spectrophotometry	20
Data Analyses	20
Results	21
Contractile Function of C57B6 and PAR2 -/- Aorta	21
Neuraminidase Effects on Contraction of C57B6 and PAR2 -/- Aorta	21
Effect of Neuraminidase Treatment on Relaxation of Phenylephrine and U46619 Precontracted Aorta	22
Neuraminidase Effect on Vasodilatory Responses in PAR2 -/- Aorta	25
Relative Serine Proteinase Activity of mMCP-7, Bovine Pancreas Trypsin and hMC β - Tryptase	26
Standardized Serine Proteinase-Mediated Relaxation Responses in C57B6 Aorta	29
Responses of C57B6 Aorta to Treatment With Serine Proteases and P20	30
Effect of Ca^{2+} -Activated K^+ Channel and NO Inhibition on Contractility of Aorta	33
PAR2 AP-Induced Relaxations of C57B6 Aorta	34
Acetylcholine-Induced Relaxations of C57B6 Aorta	35
SNP-Induced Relaxations of C57B6 Aorta	36
Discussion	38
General Findings	38
Activation of PAR2 by Serine Proteinases in C57B6 Aorta	39
SK $_{Ca}$ and IK $_{Ca}$ Interaction With NO-Mediated Relaxation in C57B6 Aorta	41
Conclusions	43
Appendix A	53

Abstract

Proteinase-activated receptor 2 (PAR2) may link inflammation with the progression of cardiovascular diseases. We examined the potential of mouse mast cell protease 7 (mMCP-7), an enzyme similar to human mast cell β tryptase (hMC β -tryptase), to activate PAR2-dependent vasodilation and the interaction of Ca²⁺-activated K⁺ channel (K_{Ca}) activation by PAR2 with eNOS-dependent relaxation in the aorta. Aortas from mice expressing PAR2 (PAR2 +/+) and PAR2 knockout (PAR2 -/-) mice were used to bioassay the PAR2 activity of mMCP-7 and PAR2-activating peptide (2fly) in the presence of inhibitors of K_{Ca}. mMCP-7 did not produce relaxation responses like hMC β -tryptase in the mouse aorta and inhibitors of K_{Ca} channels did not affect PAR2-mediated endothelial nitric oxide synthase dependent-relaxations of the aorta. These data highlight species and mechanistic heterogeneity in the ability of an orthologous enzyme agonist to activate PAR2 in different arteries. The results emphasize the need for cautious interpretations of studies assessing the pathophysiological role of PAR2 in different animal models.

Acknowledgements

This thesis was not possible without the guidance of my mentors within the Cardiovascular and Renal Sciences Group of Memorial University. Primarily, I would like to thank Dr. John McGuire for his guidance and leadership. His supervision has developed my understanding of research and challenged my mind to critical thinking which was necessary in questioning various scientific hypotheses. Secondly, I would like to thank Dr. Reza Tabrizchi, Dr. John Smeda, and Dr. Bruce Van Vliet for their knowledge and insight during development of my experiments. They have been great mentors and I am proud to have had a chance to work with them. I would also like to thank our research assistant Ms. Sarah Halfyard for her teachings and also her cheerful charm. Contributions to my thesis have also been given by Dr. Steve Compton (University of Hull). I would like to thank Steve for the expertise and ideas which he shared. Finally, my thesis would not be possible without the support of Jennifer, Callista, and especially my parents (Jim and Marilyn) who have demonstrated love and guidance during this period of my life.

Financial and infrastructure support for the research described within this thesis were made possible through grants of the Canadian Institutes of Health Research (Regional Partnership Program, ROP 72465; ROP 88065), Canada Foundation for Innovation (New Opportunities Fund, 10027), the Department of Innovation, Trade and Rural Development, Province of Government of Newfoundland (Industrial Research and Innovation Fund, 0405-017; 0506-014; 0708-022; 0708-008) and Memorial University to Dr. John McGuire.

Co-Authorship

This thesis was based on research conducted by the candidate J. Chris King, under the guidance of the primary supervisor Dr. John J. McGuire Ph.D. and the Cardiovascular-Renal Sciences Graduate Program thesis supervisory committee members Dr. John S. Smeda Ph.D. and Dr. Reza Tabrizchi Ph.D., who provided assistance with the research proposal, design and preparation of the written work.

All data were obtained and analyzed by J. Chris King using the resources provided by the laboratory and research program of Dr. John McGuire.

List of Figures

- Figure 1** - Effect of neuraminidase (45 mU/ml) on phenylephrine (n=4) contraction of the C57B6 aorta- 22 -
- Figure 2** - Effect of neuraminidase (45mU/ml) treatment on U46619 (100 nM) – induced contraction of PAR2 +/+ (n=6) and PAR2 -/- (n=3) mouse aortas- 22 -
- Figure 3** - Relaxation responses of phenylephrine-contracted C57B6 aorta by mMCP-7 (10 mU/ml), 2fly (1 μ M), and acetylcholine (100 μ M).....- 24 -
- Figure 4** - Relaxation responses of U46619-contracted C57B6 aorta by mMCP-7 (10 mU/ml), 2fly (1 μ M), and acetylcholine (100 μ M)- 25 -
- Figure 5** - Relaxation responses of PAR2 -/- aorta (n=3) by mMCP7 (10 mU/ml), 2fly (1 μ M), acetylcholine (100 μ M) and sodium nitroprusside (100 μ M).....- 26 -
- Figure 6** - Relationship between the rate of p-nitroanilide production and concentration of bovine pancreas trypsin in a solution of 1mM of BAPNA...- 28 -
- Figure 7** - Amidolytic reaction rates of bovine pancreas trypsin (10 μ g/ml), mMCP7 (50 μ g/ml), hMC β -tryptase (0.1 μ g/ml) using BAPNA (1mM) measured at 410 nM (n=3).....- 28 -
- Figure 8** - U46619 concentration-contraction response of the aorta of C57B6 mice...- 29 -
- Figure 9** - Standardized serine proteinase activity-relaxation responses for mmcp7 (10 mU/ml), bovine pancreas trypsin (10, 60, 375 mU/ml), hMC β -tryptase (10, 375, 1770 mU/ml) and hMC β -tryptase (1770 mU/ml) + neuraminidase (45 mU/ml) in U46619 (100 nM)-contracted C57B6 aorta- 30 -

Figure 10 - Relaxation responses to treatment of C57B6 aorta with trypsin
(10, 60, 375 mU/ml), hMC β -tryptase (10, 375, 1770 mU/ml), and mMCP7 (10
mU/ml) in the presence and absence of P20 peptide (5 μ M).....- 32 -

Figure 11- U46619-induced contractions of untreated (controls, n=15), NO
synthase inhibitor-treated and K_{Ca} inhibitor-treated C57B6 aorta.....- 33 -

Figure 12 - 2fly-induced relaxations of untreated (controls, n=15), NO synthase
inhibitor-treated and K_{Ca} inhibitor-treated C57B6 aorta.....- 35 -

Figure 13 - Acetylcholine-induced relaxations of untreated (controls, n=15), NO
synthase inhibitor-treated and K_{Ca} inhibitor-treated C57B6 aorta.....- 36 -

Figure 14 - SNP-induced relaxations of untreated (controls, n=15), NO synthase
inhibitor-treated and K_{Ca} inhibitor-treated C57B6 aorta.....- 37 -

List of Abbreviations

- 2fly – 2-furoyl-LIGRLO-amide
- ACh – Acetylcholine
- BAPNA – N- α -benzoyl-D, L-arginine-p-nitroanilide
- BK_{ca} – Large-conductance calcium-activated potassium channels
- CRC – Contraction response relationship curves
- cyclic GMP – 3,5 cyclic guanosine monophosphate
- ECL2 – Extracellular loop 2
- EDH – Endothelium-dependent hyperpolarization
- eNOS – Endothelial nitric oxide synthase
- IK_{ca} – Intermediate-conductance calcium-activated potassium channels
- IL - Interleukin
- hMC β -tryptase – Human mast cell β -tryptase
- L-NAME – Nitro-L-arginine methyl ester
- mMCP – Mouse mast cell protease
- NO – Nitric oxide
- PAR(s) – proteinase-activated receptor(s) or protease-activated receptors
- PAR_n – proteinase-activated receptor *n*, where *n* = 1, 2, 3 or 4
- PAR2 -/- – Proteinase-activated receptor 2 knockout mice
- PAR-AP – Proteinase-activated receptor activating peptide
- SK_{ca} – Small-conductance calcium-activated potassium channels
- SNP – Sodium nitroprusside

Introduction

Background

Proteinase-activated receptors (PARs) are members of the G protein-coupled heptahelical, transmembrane domain superfamily. There are 4 PARs: PAR1, PAR2, PAR3, and PAR4; named in the order of their protein sequence discovery (Hollenberg, 2003). PARs are expressed on many cells and are abundant throughout the cardiovascular and circulatory systems. PAR1 is expressed on platelets (Vu *et al.*, 1991), fibroblasts (Connolly *et al.*, 1996), endothelial cells, smooth muscle, and the myocardium (Hamilton *et al.*, 2002). PAR2 is expressed on the epithelium and endothelium (D'Andrea *et al.*, 1998), leukocytes (Dery *et al.*, 1998), and vascular smooth muscle (Bono *et al.*, 1997). PAR3 is expressed on medium sized arteries (D'Andrea *et al.*, 1998; Molino *et al.*, 1998), human bone marrow megakaryocytes (Ishihara *et al.*, 1997), and platelets (Kahn *et al.*, 1998). PAR4 is expressed on platelets (Ishihara *et al.*, 1997), megakaryocytes (Kahn *et al.*, 1998) and cardiomyocytes (Sabri *et al.*, 2003). Their broad expression has led to reports of many putative biological functions.

PARs are activated differently than other G-protein coupled receptors. All PARs are activated by serine proteases which cleave the N-terminus of the receptor at specific locations. This exposes specific peptide residues unique to each PAR which act as tethered ligands by interacting with their second extracellular loops, producing activated conformations. As noted in Table 1, there is no overlap between the capacity of hMC β -tryptase to activate PAR2 with PAR1, PAR3, and PAR4. Enzymatic cleavage of PAR2 by all enzyme activators exposes the amino-terminus peptide sequence SLIGRL,

Table 1. List of enzymes that recognise PAR1, PAR2, PAR3 and/or PAR4 as being substrates. Enzymes listed are serine proteinases that have been identified as being able to either activate or disarm the receptors. References are provided in the text.

PAR1	PAR2	PAR3	PAR4
Thrombin	Trypsin	Thrombin	Thrombin
Factor Xa	Human mast cell β -tryptase		Trypsin
Granzyme A	Factor VIIa		Cathepsin G
Gingipain	Factor Xa		Gingipain
	Proteinase-3		

in rodents, and SLIGVK in humans (Hollenberg, 2003). This conserved feature of PARs across species has enabled development of pharmacological tools such as PAR-activating peptides (PAR-AP) that have then been used to study the biological effects of activating PARs in many different animal models.

PAR2-activating peptides

Synthetic peptides (5-14 amino acid residues) with sequences corresponding to the revealed tethered ligand activate the PARs with the same action and subsequent signaling as serine proteinases (Schmidlin *et al.*, 2001). These peptide agonists of PARs

and several amino-terminal modified peptidic compounds are referred to as PAR-activating peptides (PAR-APs). Table 2 provides a list of PAR-AP associated with different PARs from several species. As shown in Table 2, the PAR2-AP 2fly is specific for PAR2 and is amongst the most potent agonist for PAR2 described having 10–300 times more potency than SLIGRL-NH₂ (McGuire *et al.*, 2004). 2fly was derived from 2-furoyl-LIGKV-OH which mimicked the actions of SLIGRL-NH₂ *in vivo* in a mouse model of chronic arthritis (Ferrell *et al.*, 2003). 2-furoyl-LIGKV-OH exhibited more prolonged activity in comparison to SLIGRL-NH₂. The N-terminal substitution of the serine in SLIGRL by a furoyl group may protect PAR2-AP from endogenous aminopeptidases resulting in greater bioavailability and prolonged activity. The addition of ornithine to the carboxy terminal (intended to facilitate radiolabeling) increased potency (Vergnolle *et al.*, 1998; Maryanoff *et al.*, 2001). Activating PARs with PAR-APs in animal models of diseases has provided some insight into possible cardiovascular functions of PARs *in vitro* and *in vivo*. An understanding of the mechanisms of actions of PAR-AP *in vitro* may help in determining how PARs could be used as therapeutic agents targeting the vasculature.

Table 2. Synthetic peptides for activating PAR1, PAR2, PAR3, and PAR4			
PAR1	PAR2	PAR3	PAR4
SFLLRN-NH ₂ (humans, rat, mouse)	SFLLRN-NH ₂ (human, rat, mouse)	None	GYPGQV-NH ₂ (human)
TFLLR-NH ₂	SLIGKV-NH ₂ (human)		GYPGKF-NH ₂ (mouse, rat)
TFRIFD	SLIGRL-NH ₂ (mouse, rat)		AYPGKF-NH ₂ (human)
	trans-cinnamoyl-LIGRLO-NH ₂		
	2-furoyl-LIGRLO-amide (2fly)		

PAR2 has numerous putative roles within the vasculature including regulation of blood pressure and vascular tone through endothelium-dependent smooth muscle relaxation (Cocks *et al.*, 2000; Damiano *et al.*, 1999; Hwa *et al.*, 1996; Saifeddine *et al.*, 1996; Al-Ani *et al.*, 1995), alteration of vascular permeability (Vergnolle *et al.*, 1999), protection against coronary ischemia reperfusion injury (Napoli *et al.*, 2000) and the induction of vascular smooth muscle proliferation (in cultured cells; eg. see Bono *et al.*, 1997). A specific endogenous activator of PAR2 that would be in position to physiologically activate PAR2 in the vasculature has not yet been identified, therefore the exact function of activating PAR2 remains unclear. However, the pharmacological actions of PAR2-AP on vascular smooth muscle would suggest that PAR2 activation may play an important role in modulating hemodynamics i.e. acutely lowering blood pressure

as a result of peripheral vasodilation. Indeed PAR2 knockout mice (PAR2 $-/-$) were found to have a modest blood pressure phenotype characterized by significantly increased systolic pressures (4 % higher than controls) and pulse pressures (10 % higher than controls) as measured by radiotelemetry (McGuire *et al.*, 2008).

PAR2-dependent relaxation of vascular smooth muscle

There are two mechanisms that have been reported to cause PAR2-dependent vasodilation of blood vessels; 1. Nitric oxide production and 2. Endothelium-dependent hyperpolarization (EDH) (reviewed in McGuire *et al.*, 2004). Both mechanisms are dependent on activation of PAR2 on endothelial cells that initiates increasing intracellular calcium, but there has been some heterogeneity reported about the components of the subsequent pathways.

In the first mechanism, PAR2 activation elicits an increase in intracellular calcium which results in calcium-calmodulin activation of nitric oxide (NO) synthesis by endothelial NO synthase (eNOS) through the oxidation of L-arginine to L-citrulline. NO diffuses into the adjacent smooth muscle cell where it binds to the heme active site of soluble guanylyl cyclase which catalyses production of 3,5 cyclic guanosine monophosphate (cyclic GMP) from guanosine triphosphate. Cyclic GMP accumulation activates cyclic GMP-dependent kinases that phosphorylate numerous proteins, resulting in a net effect of increasing intracellular sequestration and extrusion of calcium from the vascular smooth muscle cell (McGuire *et al.*, 2004). This mechanism is inhibited by the eNOS inhibitor L-NAME and is absent in eNOS knockout mice (McGuire *et al.*, 2002). It is the major mechanism promoting PAR2 induced vasodilation in large diameter arteries.

The second vasodilator mechanism utilized by PAR2 is independent of NO production. PAR2 promotes an increase in intracellular calcium in endothelial cells which is associated with the concurrent development of endothelium-dependent hyperpolarization in the underlying vascular smooth muscle. The common and best supported explanation for the occurrence of hyperpolarization is that calcium released from intracellular stores within the endothelium activates small- (SK_{Ca}) and intermediate- (IK_{Ca}) conductance calcium-activated potassium channels. Endothelial hyperpolarization is then conducted through myoendothelial gap junctions causing the vascular smooth muscle cell hyperpolarization (McGuire et al., 2004). Hyperpolarization of the membranes of vascular smooth muscle cells results in decreased entry of calcium through L-type calcium channels with a net lowering of intracellular calcium and vascular tone. This mechanism is blocked by selective K_{Ca} inhibitors in mice (McGuire et al., 2002; McGuire et al., 2004; McGuire et al., 2007). It is also reduced by barium (an inhibitor of inward rectifying K^+ channels) and ouabain (inhibitor of Na^+/K^+ ATPases) likely as a result of the depolarizing effects of the later compounds on the vascular smooth muscle cells (McGuire et al., 2002; McGuire et al., 2004). Reports of PAR2 mechanisms of action involving K_{Ca} have predominantly been observed in small diameter arteries.

A heterogeneous list of EDH mechanisms have been described for numerous G protein coupled receptor agonists including bradykinin and acetylcholine (reviewed in McGuire et al., 2001). Some researchers have proposed that the activation of receptors on endothelial cells (e.g. muscarinic, bradykinin) results in the release of diffusible compounds (other than NO and prostacyclin that are synthesised by endothelial enzymes) which promote vascular smooth muscle cell relaxation. In all such reports, *de novo*

compounds have been isolated after stimulation of endothelial cells with non-PAR2 based drugs that produce similar endothelium-dependent hyperpolarization of blood vessels (McGuire et al., 2001; Vanhoutte *et al.*, 2007). No one has been able to isolate a hyperpolarizing compound which has been produced by the endothelium after PAR2 stimulation. Even with the vast heterogeneity of chemical factors that have been isolated as co-called EDH factors, extending such findings to PAR2-based signals remains largely unsupported by pharmacological inhibitor studies (McGuire et al., 2002; McGuire et al., 2004; McGuire et al., 2007). Nevertheless, without exception K_{Ca} have been identified as essential components initiating endothelium-dependent hyperpolarization of vascular smooth muscle cells by PAR2.

Calcium-Activated Potassium Channels (K_{Ca})

Studies involving gene sequencing, pharmacology, and channel conductance indicate that there are three broad categories of K_{Ca} channels. Large (BK_{Ca}), intermediate (IK_{Ca}), and small (SK_{Ca}) conductance K_{Ca} channels have been identified in the vasculature. Activation of these channels may be linked to intracellular calcium levels and coupled to, or independent of, changes of membrane potential. The basic functional unit of a K_{Ca} channel is the presence of multi α -subunits that form a symmetric K^+ permeable pore (Jensen *et al.*, 2002). This complex is also the target of inhibitors.

BK_{Ca} channels are expressed in vascular smooth muscle, but are not expressed on the endothelium (Triggle, 2005). BK_{Ca} channels exhibit relatively higher single-channel conductance of approximately 250 pS compared to SK_{Ca} (5-10 pS) and IK_{Ca} channels (20-40 pS) (Vergara *et al.*, 1998). BK_{Ca} are modulated by membrane potential

depolarization and activated by increases in intracellular calcium concentration (Toro *et al.*, 1998). As a result of these characteristics, these channels are proposed to play a role in providing feedback inhibition of the activity of voltage-dependent calcium channels (i.e. to counter vasoconstriction) (Vergara *et al.*, 1998). BK_{Ca} channel pores are tetramers of α -subunits containing numerous negatively charged residues which are highly conserved among different species (Vergara *et al.*, 1998, Kamouchi *et al.*, 1999), their amino acid sequence is commonly comprised of several different splice variants of the *Slo* gene (Atkinson *et al.*, 1991, Knaus *et al.*, 1995). Four accessory β 1-subunit integral membrane proteins having two transmembrane loops form the pore. The amino- and carboxyl-terminus reside within the cell, and interact with the pore-forming tetramer. Basic channel properties such as ion selectivity and voltage-dependence are determined by α subunit composition. The interaction of the β 1-subunits modulates these properties. Deletion of the β 1-subunit uncouples BK_{Ca} channels from calcium sparks arising from the sarcoplasmic reticulum. This is proposed to increase vascular tone and contribute to hypertension (Lohn *et al.*, 2001). The co-expression of the β 1-subunit results in increased calcium sensitivity of the channel and higher intracellular calcium concentrations creating a negative shift in the voltage range of activation. (Kamouchi *et al.*, 1999). With the exception of being proposed as a vascular smooth muscle receptor for endothelial-derived arachidonic acid metabolites such as epoxyeicosatrienoic acids (EETs), BK_{Ca} activation likely does not mediate EDH mechanisms in response to agonists such as PAR2.

IK_{Ca} and SK_{Ca} are expressed on endothelial cells and are absent in vascular smooth muscle. These channels are consistently involved with EDH mechanisms (McGuire *et al.*, 2001, Vanhoutte, 2006). IK_{Ca} channels are voltage-independent and have

single channel conductance values of 30-39 pS (Jensen *et al.*, 1998). The IK_{Ca} channel gene (also referred to as SK4 gene) encodes a 427 amino acid protein with a short N-terminal component followed by a six transmembrane domain and a long C-terminal tail. Both termini are intracellularly located and the K^+ channel pore region is located between transmembrane domains five and six (Jensen *et al.*, 2001). Intracellular free calcium concentration greater than 50-100 nM is sufficient to generate a steady IK_{Ca} channel current and above such threshold these channels are open at all membrane potentials i.e. voltage independent (Jensen *et al.*, 2002). The opening of IK_{Ca} channels is triggered by calcium-bound calmodulin binding to the C-terminal of the channel (Fanger *et al.*, 1999). IK_{Ca} have been reported to co-localise to sites of intercellular calcium release at the endothelium sarcoplasmic reticulum and myoendothelial gap junctions. This localization provides an opportunity for the channels to modulate myoendothelial communication.

SK_{Ca} are encoded by SK1, SK2 and SK3 genes. The protein N- and C-termini reside within the cytoplasm and are separated by six transmembrane domains. There is a re-entrant loop between the 5th and 6th transmembrane domains that is believed to modulate selectivity and the conduction pathway for K^+ in a manner similar to that observed in IK_{Ca} . Molecular, biochemical, and electrophysiological studies have demonstrated that calcium gating in SK_{Ca} channels is promoted by heteromeric assembly of α subunits with constitutively associated calmodulin. This serves as the intrinsic calcium sensors for the channels as in the case of IK_{Ca} . Calcium-independent interactions of these channels with calmodulin promotes proper subcellular trafficking and final expression in the plasma membrane (Maylie *et al.*, 2004). The activation of the outward K^+ hyperpolarizing membrane potential currents resulting from the opening of K_{Ca} are

dependent on calcium released from the sarcoplasmic reticulum, and augment further calcium influx into the endothelium through non-selective cation channels. This allows the channels to modulate the activity of other calcium-calmodulin dependent enzymes such as endothelial NO synthase.

Characteristics of Mast Cells

Mast cells are polymorphonuclear leukocytes. These cells contain enzyme-rich lysosomes that can degrade infectious microorganisms and play an important role in immunological protection against microbial infections (Payne *et al.*, 2004). Other roles attributed to mast cells include wound healing and producing anaphylactic reactions (Thomas *et al.*, 1998, Cairns *et al.*, 2005). In the latter case, anaphylactic responses arise from the release of granules containing histamine, heparin, tryptases, and numerous cytokines from mast cells (Coico *et al.*, 2003). These substances (released upon activation of mast cells by the cross linking of immunoglobulin E antibody receptors or the activation of complement proteins) cause a localised increase in blood flow and a leakage of fluid (edema) and plasma proteins into the tissue. This causes an inactivation of antigenic agents, sometimes at the consequences of disrupting pathological organ function (Guyton, 2006). These compounds also activate sensory neurons increasing the perception of pain (nociception) that is associated with inflammatory reactions (Barbara *et al.*, 2007). Human mast cells are distinguished phenotypically by different anatomical locations (mucosal versus connective tissue) and neutral proteases (characterized by their electrophoresis isoelectric point). Mucosal mast cells contain mostly tryptases, while connective tissue mast cells found in the parenchyma of the lungs or within skin layers

contain tryptases, chymases and carboxypeptidases (Cairns, 2005). Numerous substances released by mast cells have been assessed with respect to their involvement in inflammatory responses within the cardiovascular system.

Tryptase

Tryptases are serine proteases released from mast cells that cause microvascular leakage and inflammation during allergic reactions (Yoshinori *et al.*, 2005). Basophils (the only other cell type known to contain tryptases) have significantly lower levels of tryptases than mast cells (Castells *et al.*, 1987). Tryptases hydrolyze peptide bonds on the carboxy-terminus of basic residues. The difference between tryptases and trypsin activity relates to the ideal/preferred sequences that are 3 amino acids upstream and 3 amino acids downstream of the hydrolysed bond of potential substrates. The 5 tryptases isolated from humans are named α , β , γ , δ and ϵ forms (Cairns, 2005). While sharing a common family name, each tryptase form has unique substrate selectivity. The β -form has little overlap in preferred substrates with the other tryptases (which have chymase activity) and has a unique 3 dimensional structure. Since it is the only tryptase known to activate PAR2 it will be the focus of further discussion.

β -tryptase is the most abundant tryptase in mast cells. Its concentration varies depending upon the location; 35 pg in mast cells located in connective tissue and 12 pg in mast cells located in mucosal (lung) tissue (Cairns, 2005). Concentrations of β -tryptase are increased in systemic anaphylaxis and other hypersensitivity allergic reactions (asthma, interstitial lung disease, and rheumatoid arthritis). Baseline values in asthmatics are reported as being 2 ng β -tryptase per ml of lavage fluid, which are significantly higher than what is found in non-asthmatic humans (Cairns, 2005). β -tryptase up-regulates IL-1 β

and IL-8 secretion, enhances the presence of intracellular adhesion molecules/selectins on endothelial cells, mediates accumulation of neutrophils and eosinophils, produces vascular leakage, and is mitogenic for epithelial cells, fibroblasts, and smooth muscle cells in culture (Steinhoff *et al.*, 2005).

Human mast cell β -tryptase (hMC β -tryptase) is a tetramer protein that is stabilised by negatively charged heparin proteoglycans. Upon dissociation of heparin, the tetramer separates into monomers that are not associated with tryptase-specific catalytic activity (Cairns, 2005). The crystal structure of β -tryptase consists of a flat-ringed frame formed by four monomers which surround a narrow central pore. This pore contains four catalytic sites, each facing inward from the walls of the frame. The pore size restricts entry of large substrates and proteinase inhibitors into the catalytic sites (Pereira *et al.*, 1998). Endogenous β -tryptase inhibitors have been isolated. It is thought that the dissociation of β -tryptase into monomers is the normal rate-limiting event to its activity. In mice, two orthologous isoforms of human β -tryptase have been proposed, mMCP-6 and mMCP-7. Both of these murine enzymes are located on chromosome 17 and each features an apparent tetramer composition and similar substrate selectivity as the human β -tryptase (Gurish *et al.*, 1993; Gurish *et al.*, 1994). Discovering the substrate targets of mMCP-7 and mMCP-6 will provide information about their roles in inflammation.

PAR2 and human mast cell β -tryptase relationship

hMC β -tryptase has been shown to cleave PAR2 receptors on human epithelial and endothelial cells in culture (Molino, 1997). PAR2 expressed on rat colonic myocytes, keratinocytes, and guinea-pig myenteric neurons can be activated by β -tryptase (Compton *et al.*, 2001). hMC β -tryptase has been proposed to link elevated mast cell levels with

PAR2 activation during inflammation, hypersensitivity reactions and wound repair. It is thought that PAR2 activation could stimulate the immune response by producing endothelial cytokines and adhesion molecules, a response demonstrated to occur in cell culture studies. If such events are linked then a PAR2 agonist may be therapeutically used to block inflammatory reactions.

hMC β -tryptase (both the recombinant and purified from human lung forms) degrade neuropeptides such as vasoactive intestinal peptide and calcitonin gene-related peptide, which are capable of influencing smooth muscle tone (Cairns, 2005). Fajardo *et al.* (2003) reported that hMC β -tryptase is also a potent gelatinase and such activity may contribute to connective tissue degradation associated with diseases such as rheumatoid arthritis, independent of PAR2 activation.

Glycosylation of PAR2

All four members of the PAR family contain N-linked glycosylation sites as do most heptahelical G protein-coupled receptors. Human PAR2 encodes 2 sites, 1 on extracellular loop 2 (ECL2) and the other on the receptor N-terminus. The critical role of the glycosylation site on ECL2 for PAR2 signalling was demonstrated by Lerner *et al.* (1996) splicing ECL2 of PAR2 into PAR1 and he demonstrated PAR2-specificity for ligand recognition within ECL2. Compton *et al.* (2002) showed that PAR2 N-linked glycosylation regulates both receptor expression and signalling. Mutations of the N-terminus sequence of human PAR2 and sialic acid-deficient human PAR2 produced increased sensitivity in response to β -tryptase activation. It was postulated that glycosylation serves to reserve the activation of PAR2 for events associated with pathogenic invasion. Under conditions where sialidases are secreted and remove the N-

linked sugars, PAR2 could play a role in mediating responses between the immune and vascular system when immune cells recruited to the site of injury release the serine proteinases such as β -tryptase.

PAR2 and inflammation

A link between PAR2 and inflammation has been supported by many studies. PAR2 expression is up-regulated by pro-inflammatory mediators such as tumour necrosis factor α , interleukin 1β (IL- 1β) and lipopolysaccharide in cell cultures (Nystedt *et al.*, 1996). PAR2 gene deletion in mice produces a protective phenotype against various diseases (arthritis, asthma, colitis) (Schmidlin *et al.*, 2002; Ferrell *et al.*, 2003; Lindner *et al.*, 2000). Acute activation of PAR2 by injection of PAR2-AP into rat paws, increases vascular permeability, granulocyte infiltration, leukocyte adhesion and pain which is consistent with the enhancement of inflammation (Cocks *et al.*, 2000; Vergnolle *et al.*, 2001; Coughlin *et al.*, 2003). PAR2 activation also increases the release of prostanoids and cytokines including IL-6 and IL-8 in epithelial and non-epithelial cells (Lourbakos *et al.*, 2001). PAR2 agonists (PAR2-AP, trypsin, hMC β -tryptase) produce edema, granulocyte infiltration and increased intestinal permeability within the colon (Cenac *et al.*, 2002). The expression of PAR2 and its activation are implicated with the activation of the immune system.

In contrast to the pro-inflammatory effects of PAR2, this receptor may also play a protective role against some diseases. In the respiratory system of mice, the intranasal delivery of PAR2-AP inhibited hyperreactivity and the antigen-induced infiltration of eosinophils (De Campo *et al.*, 2005). Administering PAR2 agonists protected against experimental colitis induced by trinitrobenzene sulfonic acid. This protection, mediated

by a neurogenic mechanism, was diminished by a calcitonin gene-related peptide receptor antagonist (Fiorucci *et al.*, 2001). In the gastrointestinal tract, PAR2 agonists inhibit the formation of gastric ulcers induced by ethanol and indomethacin (Kawabata *et al.*, 2002). PAR2-AP infusion exerts a protective effect against experimental myocardial ischemia-reperfusion injury in rats. It enhances myocardial contractile recovery and decreases oxidative stress during reflow at the ischemic risk zone (Napoli *et al.*, 2000). PAR2-AP mediated vasodilation of basilar arteries in spontaneously hypertensive rats (SHR), middle cerebral arteries of pre- and post-stroke stroke prone-SHR and the mesenteric arteries of spontaneously hypertensive mice is preserved under conditions where endothelial dysfunction to other endothelial receptors exists (Sobey *et al.*, 1999; Smeda *et al.*, 2007; McGuire *et al.*, 2007). In mesenteric arteries, endothelial dysfunction was associated with a reduction in endothelial nitric oxide-mediated vasodilation and the persistent PAR2 vasodilation produced K_{Ca} -mediated vascular smooth muscle hyperpolarization (McGuire *et al.*, 2007). Such findings illustrate that the pathophysiological impact of PAR2 and its activation by serine proteinases varies with the surrounding conditions.

Rationale, Hypothesis, Objectives

hMC β -tryptase activates human and rodent PAR2. Mouse mast cell protease 7 (mMCP-7) has similar peptide substrate selectivity and structure to hMC β -tryptase. The ability of mMCP-7 to activate mouse PAR2 in intact target tissues has never been demonstrated. Such information would enhance our understanding of the relationship between PAR2 and its endogenous serine proteinase activators in mouse models of human diseases.

Our first hypothesis (hypothesis 1) was that mMCP-7 would activate PAR2 in the mouse aorta. Activation of PAR2 causes endothelium-dependent vascular smooth muscle relaxation. If mMCP-7 activated PAR2 it was expected that mMCP-7 would cause relaxation of contracted mouse aorta. We tested this hypothesis by determining the effect of recombinant mMCP-7 on isometric contracted mouse aorta. Isometric tension recordings of contracted aorta from PAR2-expressing mice (C57B6) and PAR2 knockout mice (PAR2 $-/-$) were used to bioassay PAR2 activation by mMCP-7 in the presence and absence of a deglycosylation enzyme (neuraminidase). Control responses for endothelial PAR2 activation in response to mMCP-7 were compared to those of other PAR2 agonists (trypsin, β -tryptase and 2fly), and the endothelial-dependent vasodilator acetylcholine using isometric tension recordings.

PAR2 activation can cause NO- and SK_{Ca}/IK_{Ca}-dependent vasodilation. While the endothelium of aorta expresses SK_{Ca} and IK_{Ca}, inhibition of eNOS totally blocks PAR2-AP induced vasodilation.

Our second hypothesis (hypothesis 2) was that the PAR2-AP 2fly promotes the activation of eNOS causing NO-dependent vasodilation through the activation of SK_{Ca} or IK_{Ca}. We tested hypothesis 2 by determining the effects of apamin (SK_{Ca} inhibitor) and TRAM-34 (IK_{Ca} inhibitor) on PAR2-AP, ACh- and SNP-induced relaxation in the mouse aorta. The results of these experiments should further our understanding of the mechanisms associated with PAR2 activation of large conduction arteries in mice.

Methods and Materials

Animals

Male mice 8-16 weeks of age purchased from the Jackson Laboratory (Bar Harbor, Maine, USA) were used. In the mMCP-7 studies testing hypothesis 1, C57B6 (n=18) and PAR2 -/- (n=6) mice were sacrificed at 14-18 weeks of age. In studies assessing the effects of SK_{Ca} and IK_{Ca} inhibitors used to test hypothesis 2, C57B6 (n=20) mice were sacrificed at 21-24 weeks of age. The procedures were approved by the Institutional Animal Care Committee of Memorial University and followed the principles and guidelines of the Canadian Council of Animal Care.

Materials

2-furoyl-LIGRLO-amide (2fly) was purchased from Peptides International (Louisville, Kentucky USA). TRAM-34 was purchased from Toronto Research Chemicals (North York, Ontario). Recombinant mouse mast cell protease 7 (mMCP-7) was purchased from R&D systems (Minneapolis, Minnesota, USA). P20 peptide (³⁰GPNSKGR/SLIGRLDTP⁴⁵-YGCG) was a gift from Dr. Morley Hollenberg at the University of Calgary (Alberta). Isolated, purified hMCβ-tryptase was a gift from Dr. Steven Compton at the University of Hull (Hull, UK). All other chemicals used were purchased from Sigma Aldrich Canada (Oakville, Ontario).

Measurements of isometric tension in aorta of mice

The thoracic aorta (2 mm lengths) was isolated surgically from each mouse killed by cervical dislocation. Each artery was cleaned of adherent fat and then placed between

a fixed support micropositioner and force transducer by 40 μm diameter tungsten wire in a 610M myograph chamber (Danish Myo Technology, Aarhus, Denmark) filled with Krebs solution (pH 7.4, 9 ml) comprised of 114 mM NaCl, 4.7 mM KCl, 0.8 mM KH_2PO_4 , 1.2 mM MgCl_2 , 2.5 mM CaCl_2 , 11 mM D-glucose, 25 mM NaHCO_3 and bubbled with 95% O_2 / 5% CO_2 . For each artery, the diameter at resting (baseline) tension was set to 90% of the diameter that was estimated to produce wall stress equivalent to 120 mmHg (Mulvany *et al.*, 1977). All drug solutions were applied directly to the myograph chambers (the dilution factor of stock solutions ranged from 1/100 to 1/1000), and the isometric tension changes were recorded continuously thereafter to a PC using Danish MyoDaq and ADI instruments Chart software. Flowcharts are provided (Appendix A) to outline the experimental design of drug treatment comparisons for hypothesis 1 and 2.

In all experiments, aortic segments from mice were excluded from analyses if initial contractions in response to a single test dose of 120 mM KCl did not produce a >2 mN increase in force from baseline. Following washout of KCl, U46619 (a thromboxane A_2 agonist) concentration-contraction response relationships (CRC) (0.1 nM – 1 μM) were determined for each segment of aorta. From each CRC a concentration of contractile agonist that produced 70-85% of the maximum observed was determined for each segment and used to pre-contract arteries when determining relaxation responses to compounds (next section).

In the experiments assessing hypothesis 1, relaxation responses to acetylcholine (100 μM ACh) of untreated (controls) and α 2-3, 6, 8-neuraminidase (40 min)-treated C57B6 (controls) and PAR2 $-/-$ mice arteries contracted sub-maximally by U46619 (30

nM-100 nM) were recorded to assess the state of endothelium-dependent vasodilator capacity. Arteries that did not relax to ACh were excluded from studies. Then, after each aortic segment was allowed to re-establish its contracted tension levels, mMCP-7 (10 mU), 2fly (1 μ M), hMC β -tryptase (10 mU, 375 mU, 1770 mU) or bovine pancreas trypsin (10 mU, 60 mU, 375 mU) were added in order to test the PAR2 activatable-relaxation responses. Arteries were then washed with Krebs solution to baseline and once again contracted submaximally prior to testing the relaxation response to SNP (10 μ M). In a small number of experiments in order to test whether the N-terminus containing the tethered ligand sequence of PAR2 could be cleaved by serine proteinases, P20 peptide (³⁰GPNSKGR/SLIGRLDTP⁴⁵-YGCG; 5 μ M) was added after tension recovery (if applicable) to exposure to trypsin, hMC β -tryptase or mMCP-7. When P20 is cleaved as a substrate by trypsin-like serine proteases (at R/S) the PAR2 activating sequence SLIGRL is produced. Thus, P20 peptide can be used to confirm the ability, if any, of serine proteases to recognize the PAR2 activation motif within the N-terminus.

In experiments assessing hypothesis 2, ACh, 2fly and SNP concentration-relaxation response relationships (in randomly assigned orders) were constructed in C57B6 (controls) mouse arteries contracted submaximally by U46619 (30 nM-100 nM). After a washout period (30 – 60 min) with Krebs solution, the effects of inhibitors of NO synthase (nitro L-arginine methylester; L-NAME 100 μ M), SK_{Ca} (apamin; 1 μ M) and IK_{Ca} (TRAM-34; 1 μ M, 10 μ M) were determined by exposing arteries to the inhibitors for 15 minutes prior to the random application of either ACh, 2fly, or SNP.

Measurement of the relative serine proteinase activity of purified mMCP-7, hMC β -trypsin and bovine trypsin by absorbance spectrophotometry

To compare the relative amount of serine proteinase activity which was added to myograph chambers when exposing arteries to mMCP-7, hMC β -trypsin and bovine pancreas trypsin, the amidolytic catalysis of a non-selective substrate by each preparation of enzyme was assayed. A Beckman DU series 500 single cell module spectrophotometer was used with a 100 μ l (maximum volume) glass cuvette (1 cm light path) filled with 90 μ l of the substrate N-a-benzoyl-D, L-arginine-p-nitroanilide (BAPNA; 1 mM) and 10 μ l of the test enzyme preparation. The amidolytic activities of mMCP-7 (50 μ g/ml), bovine trypsin (1, 5, 10, 25, 35, 50 μ g) and hMC β -trypsin (1 nM) were calculated from the rate of product (p-nitroanilide) formed, as measured by the change in absorbance at a wavelength of 410 nm every 15 seconds over a 20 min period. The spectrophotometry blank (zero) contained 1 mM BAPNA solution dissolved in dimethyl sulphoxide solution. An extinction coefficient for p-nitroanilide of 8800 L mol⁻¹ cm⁻¹ was used for calculation of product formation. 1 mU = amount of enzyme that produced a reaction rate of 1 nmol p-nitroanilide /min from BAPNA. Enzyme activity is therefore expressed as 'Relative BAPNA units (x 1e⁻³)'.

Data Analyses

Unless otherwise indicated the values reported are mean \pm standard error of mean (error bars on graphs; sem). The n values represent the number of mice sampled. Maximal effect (E_{max}) of U46619 was expressed as a percentage of the contraction by

120 mM KCl. E_{max} for each vasodilator was expressed as percent relaxation: 100% relaxation = complete reversal of agonist-induced contracted tone. Sensitivity is expressed by pD_2 values (negative logarithm of the concentration of agonist which produced 50% of its E_{max}). Statistical calculations were run using Microsoft Excel 2003, and Graph Pad Prizm version 4. One-way analysis of variance (ANOVA) corrected for multiple comparisons by Student Neuman Keuls post-hoc test was used to compare variables between groups of 3 or more treatments. Results were considered significantly different at $P < 0.05$.

Results

Contractile Function of C57B6 and PAR2 -/- aorta

Isometric contractions of aortic segments induced by 120 mM KCl as a relative measure of viability were not different between C57B6 (6.1 ± 0.3 mN; $n = 6$) and PAR2 -/- (5.5 ± 1.4 mN; $n=3$).

Neuraminidase effects on contraction of C57B6 and PAR2 -/- aorta

It was possible that deglycosylation treatment of tissues would be a prerequisite for mMCP-7 activation of PAR2, but this could have caused a confounding effect on the contractility of the tissues. To determine if the deglycosylation treatment like that used by Compton et al. (2002), would affect contractile function, aorta from C57B6 and PAR2 -/- were exposed to neuraminidase prior to contraction with agonists. Contractions by phenylephrine and U46619 of neuraminidase-treated aorta of C57B6 and PAR2 -/- mice were not different than contractions of untreated (controls) aorta when standardized to 120 mM KCl (Figures 1 and 2).

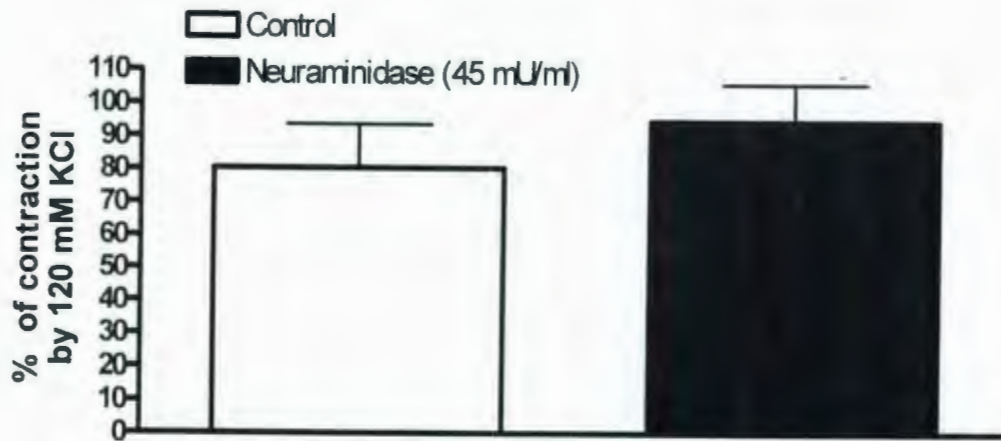


Figure 1 – Effect of neuraminidase (45 mU/ml) on phenylephrine (n=4) contractions of the C57B6 aorta. Values are mean \pm sem.

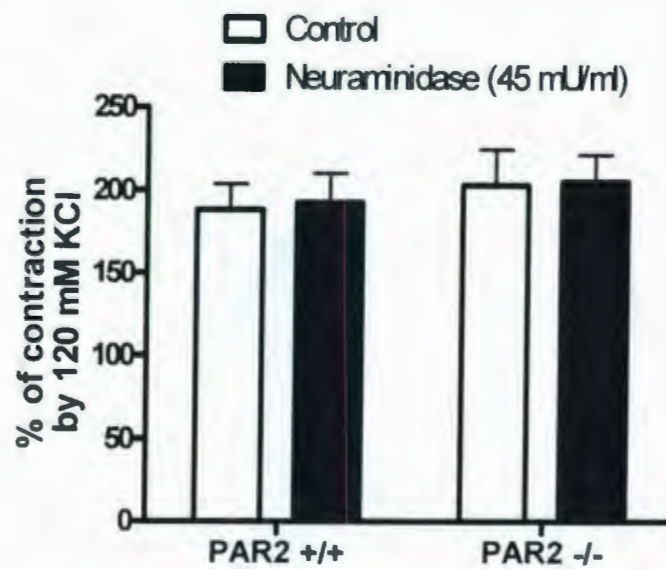


Figure 2 – Effect of neuraminidase (45 mU/ml) treatment on U46619 (100 nM) – induced contraction of the C57B6 (n=6) and PAR2 -/- (n=3) mouse aortas. Values are mean \pm sem.

Effect of neuraminidase treatment on relaxation of phenylephrine and U46619 precontracted aorta

To bioassay mMCP-7 activation of mouse PAR2, untreated and neuraminidase-treated C57B6 aortas were contracted by phenylephrine and then the relaxation responses to addition of mMCP-7 were recorded. This approach was also repeated in U46619-treated aorta in order to compare the effects of different contractile agonists on relaxations. 2fly- and acetylcholine-induced relaxation responses were used as controls to compare the effects of mMCP-7 to PAR2 and muscarinic endothelial-dependent relaxation.

mMCP-7 did not cause any relaxation (not different than 0) of either control or neuraminidase-treated C57B6 aorta that were precontracted by phenylephrine (Figure 3) or U46619 (Figure 4). In both phenylephrine- (Figure 3) and U46619- (Figure 4) contracted aortas, 2fly and ACh relaxations of C57B6 aorta were unaffected by prior neuraminidase treatment.

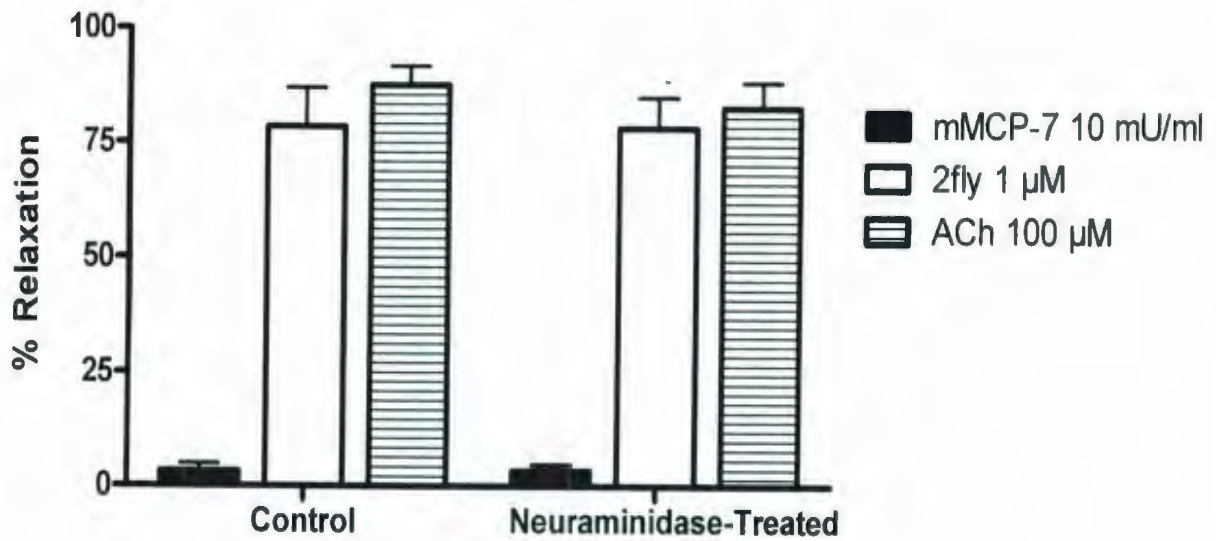


Figure 3 – Relaxation responses of phenylephrine-contracted C57B6 aorta by mMCP-7, 2fly, and acetylcholine. Aorta were either untreated (controls; n=6) or treated with neuraminidase (45 mU/ml; n=5) prior to contraction submaximally by phenylephrine (1 μM). Values are mean ± sem.

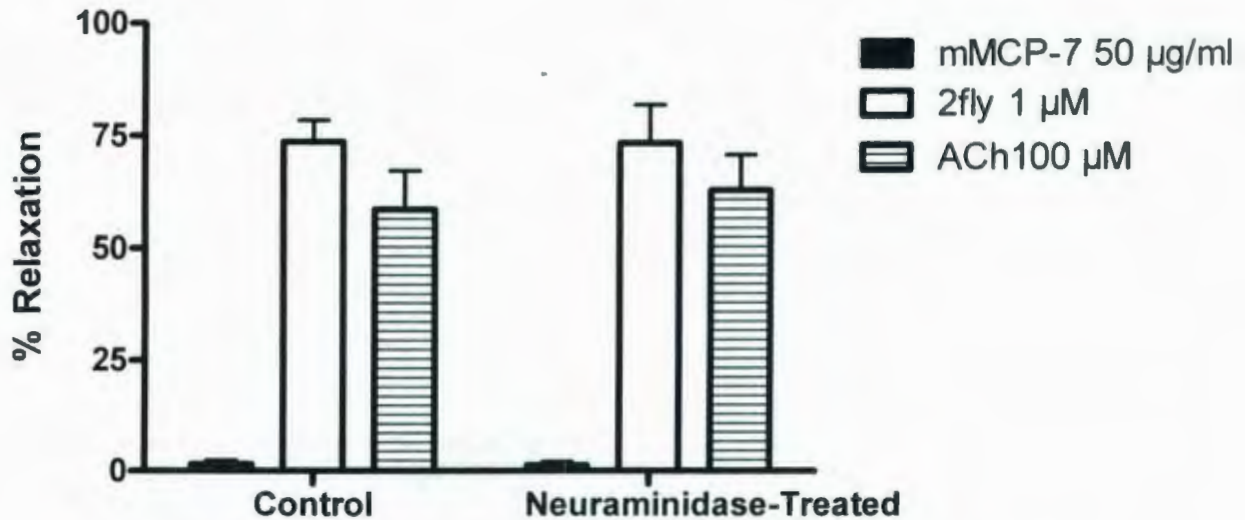


Figure 4 – Relaxation responses of U46619-contacted aorta by mMCP-7 (10 mU/ml), 2fly (1µM) and acetylcholine (100 µM). Aorta were either untreated (controls, n =5) or treated with neuraminidase (45 mU/ml, n=7) prior to contraction submaximally by U46619 (100 nM). Values are mean ± sem.

Control and neuraminidase effect on vasodilatory responses in PAR2 -/- aorta

To demonstrate the specificity of mMCP-7 and 2fly for the PAR2 receptor, U46619 was used to contract the aorta of PAR2 -/- mice and then the responses to mMCP-7, 2fly, acetylcholine and sodium nitroprusside were tested in control and neuraminidase-treated tissues. Neither mMCP-7 nor 2fly produced relaxation responses in control and neuraminidase-treated tissues sampled from PAR2 -/- mice (Figure 5). Acetylcholine and SNP-induced relaxation responses did not differ between control and

neuraminidase-treated tissues nor were these different than those observed in C57B6 aorta.

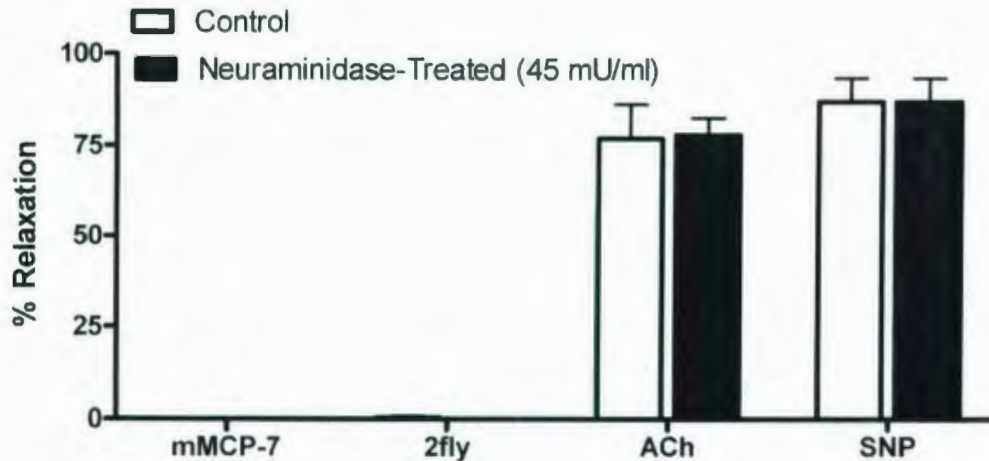


Figure 5 – Relaxation responses of PAR2 $-/-$ aorta ($n=3$) by mMCP-7 (10 mU/ml), 2fly (1 μ M), acetylcholine (100 μ M) and sodium nitroprusside (100 μ M). Untreated (controls) and neuraminidase-treated (45 mU/ml) PAR2 $-/-$ aorta were contracted by 100 nM U46619 prior to determining relaxation responses. Values are mean \pm sem.

Relative serine proteinase activity of mMCP-7, bovine pancreas trypsin and hMC β -trypsin

To compare vascular responses to different enzymes it was necessary to develop a standardization protocol to calculate the equivalent amounts of enzyme to bioassay with aorta. Enzyme activities of mMCP-7, hMC β -trypsin and bovine pancreas trypsin were measured using a common substrate BAPNA (1 mM). Figure 6 illustrates a linear relationship between rate of product formation and trypsin concentration using 1 mM BAPNA. Figure 7 shows the different amounts of each enzyme that were required to produce the equivalent rates of enzyme activity using 1 mM BAPNA. For reference of

our studies to previous reports, 2 mU of activity was defined by the rate of p-nitroanilide produced by 1 nM bovine pancreas trypsin with 1 mM BAPNA.

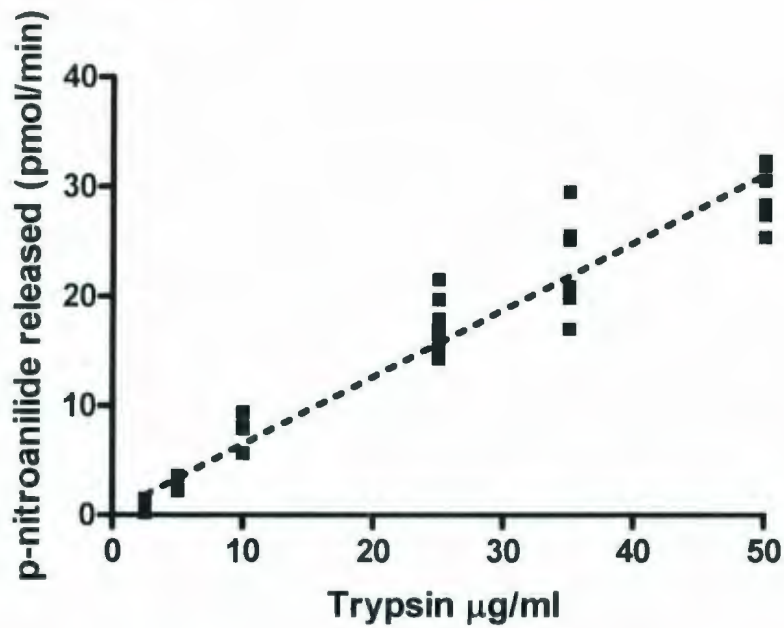


Figure 6 – Relationship between the rate of p-nitroanilide production and concentration of bovine pancreas trypsin in a solution of 1mM of BAPNA. The dashed line represents the linear regression analyses of n=8 experiments. Values are mean \pm sem.

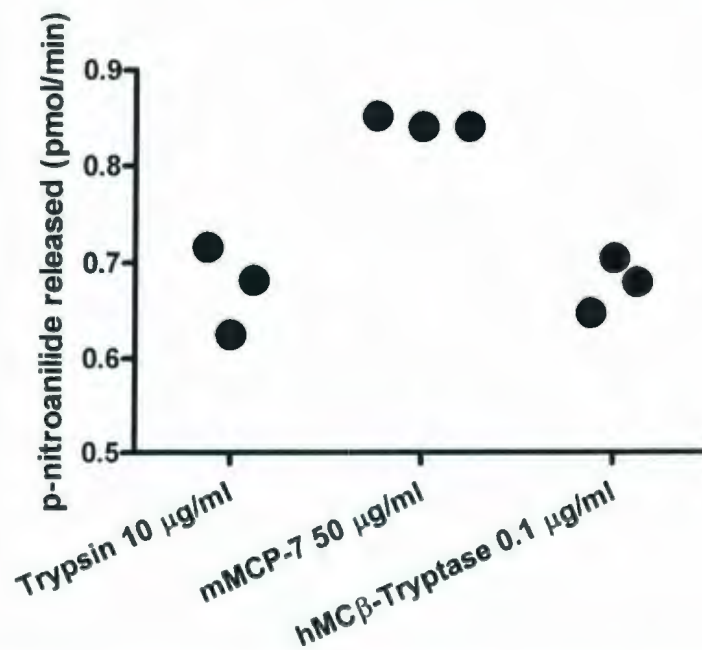


Figure 7 – Rate of p-nitroanilide production by bovine pancreas trypsin (10 µg/ml), mMCP-7 (50 µg/ml), hMCP-tryptase (0.1 µg/ml) using BAPNA (1 mM). Each symbol is a replicated sample. Values are mean \pm sem.

Standardized serine proteinase-mediated relaxation responses in C57B6 aorta

Using the standardisation protocol mentioned previously to add equivalent proteinase activity, PAR2 relaxation activity by mMCP-7, hMC β -tryptase and bovine pancreas trypsin were compared. The aortas were contracted sub-maximally as determined from U46619 concentration-contraction relationship (Figure 8). 2fly (1 μ M) and acetylcholine (100 mM) respectively caused $85 \pm 1\%$ and $80 \pm 3\%$ relaxation in U46619 (100 nM)-contracted C57B6 aorta (n=3).

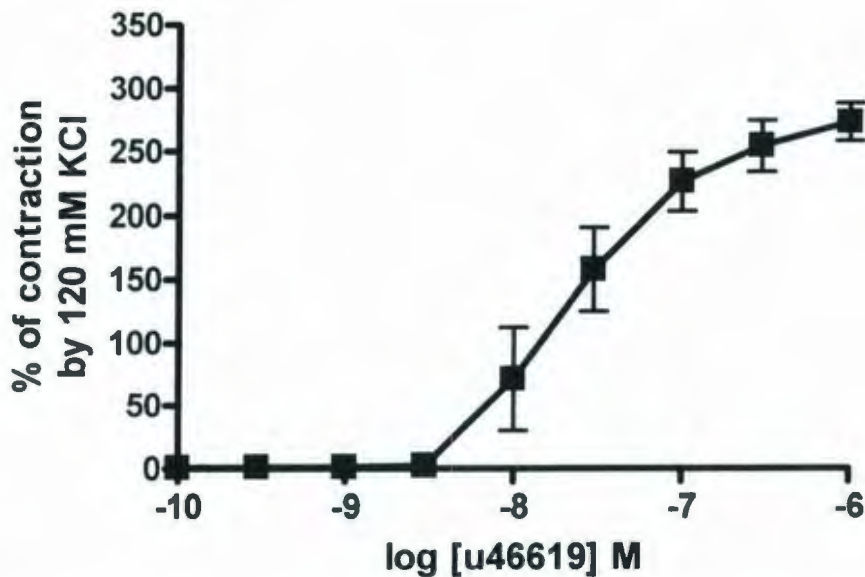


Figure 8 – U46619 concentration-contraction relationship in the aorta of C57B6 mice.

Symbols (n=3) represent the mean \pm sem. 120 mM KCl contracted aorta (n=7) by 6.3 ± 0.3 mN from resting tension.

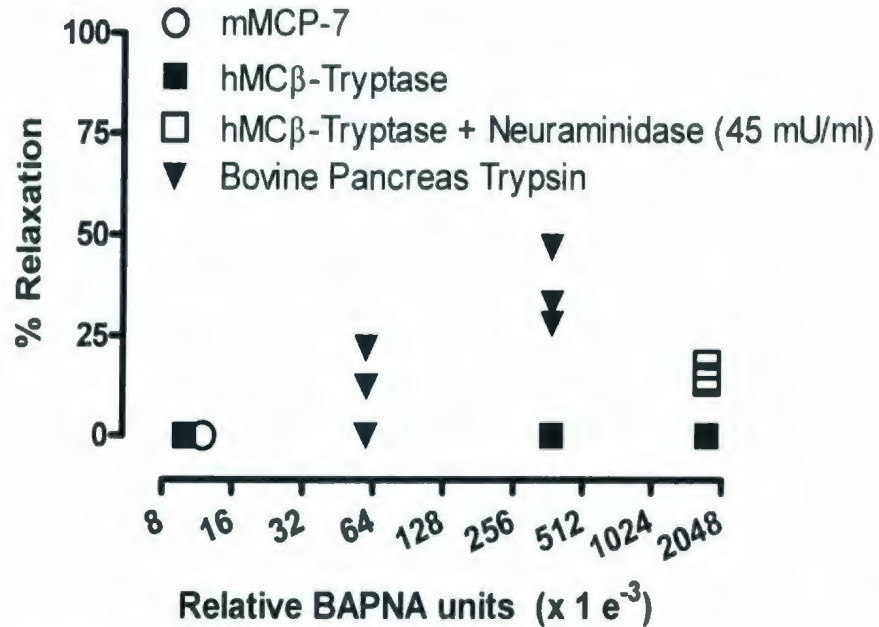


Figure 9 – Standardized serine proteinase activity-relaxation response relationships for mMCP-7, bovine pancreas trypsin, hMCP β -tryptase and hMCP β -tryptase + neuraminidase in U46619-contracted C57B6 aorta. Symbols represent the replicated responses. For clarity mMCP-7 (n=3) was nudged-rightward along the x-axis by 4 units. Control (untreated) replicate values of hMCP β -tryptase overlap at 0% (n=3).

10 mU/ml of trypsin (0%), hMCP β -tryptase (0%), and mMCP7 (0%) failed to induce significant relaxation in the C57B6 aortas. The application of 60 mU/ml and 375 mU/ml of trypsin produced significant relaxation responses $12 \pm 6\%$ and $36 \pm 6\%$ respectively. Alone, hMCP β -tryptase (375, 1770 mU/ml) did not induce relaxation response in the C57B6 aorta. Prior treatment of the C57B6 aorta with neuraminidase was required to induce relaxation response with 1770 mU/ml of hMCP β -tryptase ($16 \pm 1\%$) (Figure 9) In data not shown, the addition of 2fly after exposure to mMCP-7 produced similar relaxation responses to untreated aorta.

Responses of C57B6 aorta to treatment with serine proteases + P20

The buffer conditions within the myograph chambers may have reduced the activity of the exogenously added serine proteinases. To further test this possibility the aorta were exposed to a peptide corresponding to the N-terminus sequence of PAR2 (P20) after the addition of the various enzymes (Figure 10). P20 peptide added directly to pre-contracted C57B6 aorta in the absence of enzyme did not elicit any response. While different amounts of mMCP-7, trypsin and hMC β -tryptase were added in combination with P20, only P20 peptide added after the recovery of an elicited relaxation by 375 mU/ml bovine pancreas trypsin ($16 \pm 5\%$) caused another relaxation of C57B6 aorta (Figure 10).

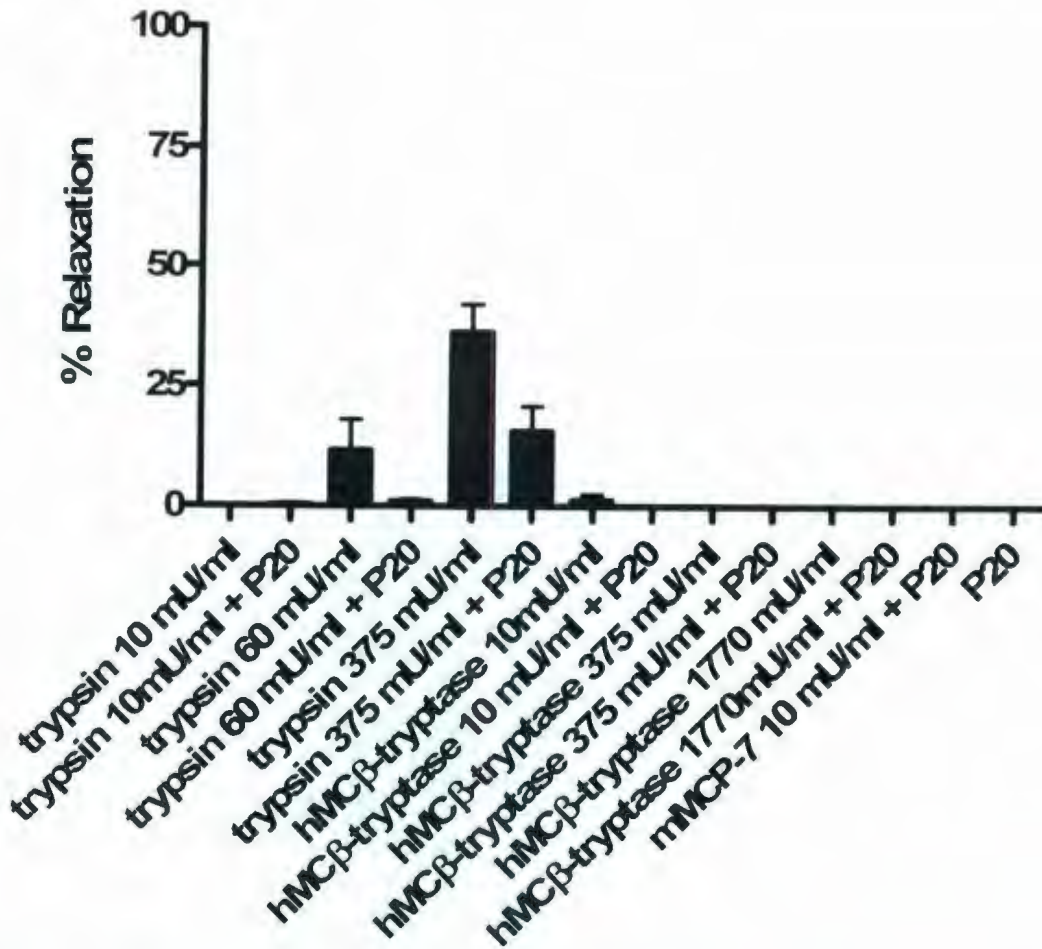


Figure 10 – Effects of P20 ± serine proteases on the C57B6 aorta. Relaxation of the C57B6 aorta by trypsin, hMCPβ-tryptase and mMCP7 in the presence and absence of P20 (5 μM).

Values are mean ± sem.

Effect of Ca^{2+} -activated K^+ channel and NO inhibition on contractility of aorta

U46619 dose response curves were standardized to 120 mM KCl (Figure 11; 6.6 ± 0.4 mN; $n=20$) in C57B6 aorta. Concentration-contractile response relationships of inhibitor-treated tissues did not differ from control tissues (E_{\max} and pD_2 : control: $246 \pm 10\%$; 7.7 ± 0.1 ; $n=15$; TRAM-34 (1 μM): $250 \pm 15\%$; 7.8 ± 0.2 ; $n=7$; L-NAME (100 μM): $242 \pm 10\%$; 8.2 ± 0.1 ; $n=7$; TRAM-34 (10 μM): $226 \pm 8\%$; 7.6 ± 0.1 ; $n=13$; TRAM-34 (10 μM) and apamin (1 μM): $227 \pm 6\%$; 7.5 ± 0.1 ; $n=14$).

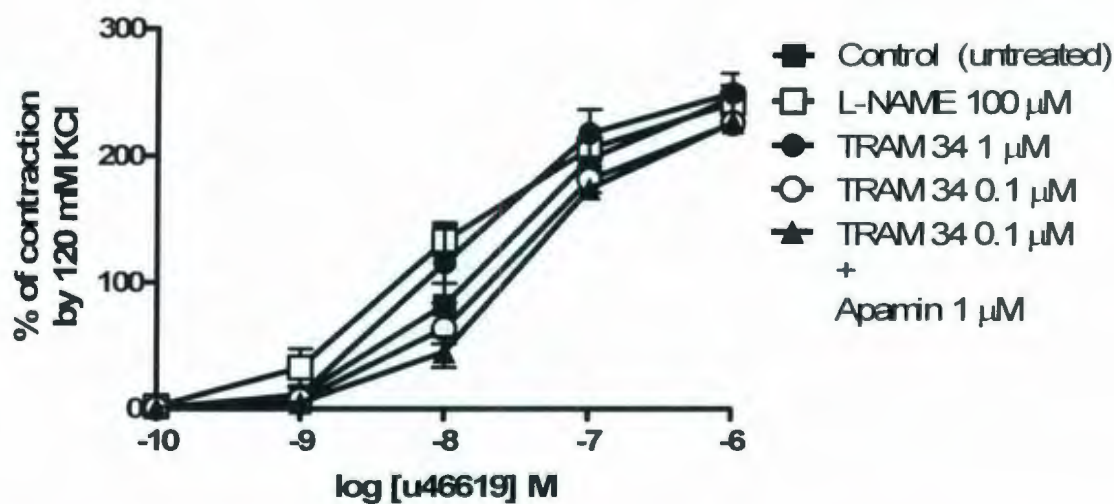


Figure 11 – Effects of L-NAME and K_{Ca} inhibitor on U46619-induced contractions of mouse aorta. Untreated (controls; $n=15$), L-NAME ($n=7$), TRAM-34 (IK_{Ca} inhibitor; 1 μM , $n=7$; 10 μM , $n=13$) or TRAM-34 + apamin (SK_{Ca} inhibitor; $n=14$)-treated aorta were contracted by cumulative addition of U46619. Values are mean \pm sem.

PAR2 AP-induced relaxations of C57B6 aorta

To test the effects of NO synthase and K_{Ca} inhibition on PAR2-mediated relaxation, C57B6 aortas were left untreated (controls) or treated with inhibitors prior to measuring 2fly-induced relaxations of U46619 pre-contracted aorta. 2fly induced relaxation was reduced by 80% in tissues incubated with an inhibitor of NO synthase (100 μ M L-NAME) compared to controls. TRAM-34 in the presence or absence of apamin did not alter 2fly mediated relaxation responses (Figure 12). The potency of 2fly mediated relaxation between controls and all K_{Ca} inhibitor groups did not differ (E_{max} and pD_2 : control: $82 \pm 2\%$; 7.6 ± 0.1 ; $n=15$; TRAM-34 (1 μ M): $74 \pm 6\%$; 7.7 ± 0.2 ; $n=7$; TRAM-34 (10 μ M): $83 \pm 4\%$; 8.0 ± 0.1 ; $n=13$; TRAM-34 (10 μ M) + apamin (1 μ M): $84 \pm 2\%$; 7.7 ± 0.1 ; $n=14$). L-NAME reduced E_{max} to $16 \pm 4\%$ but did not significantly alter pD_2 (7.3 ± 0.2 %) when compared to the control group

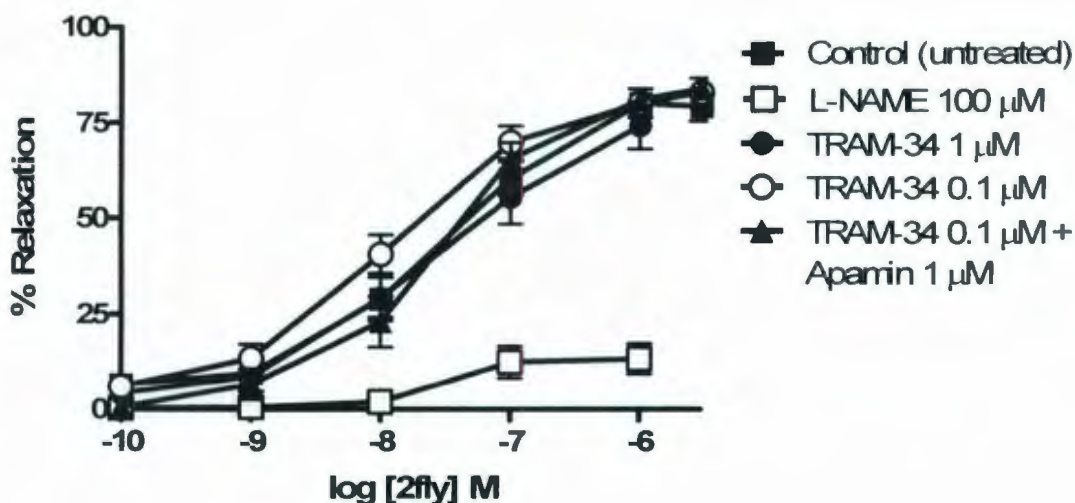


Figure 12 – Effect of K_{Ca} inhibitor on 2fly-induced relaxations of mouse aorta. Untreated (controls; $n=15$), L-NAME ($n=7$), TRAM-34 (IK_{Ca} inhibitor; $1 \mu M$, $n=7$, $10 \mu M$, $n=13$) or TRAM-34 + apamin (SK_{Ca} inhibitor; $n=14$)-treated aorta were contracted by U46619 (100 nM) prior to obtaining responses to 2fly. Values are mean \pm sem.

ACh-induced relaxations of C57B6 aortas were reduced by $\sim 95\%$ in tissues incubated with $100 \mu M$ L-NAME compared to controls and all other K_{Ca} inhibitor groups (Figure 13). Potency of ACh did not differ between controls and K_{Ca} inhibitor treatments (E_{max} and pD_2 : control: $76 \pm 4\%$; 8.2 ± 0.1 ; $n=15$; TRAM-34 ($1 \mu M$): $77 \pm 2\%$; 8.2 ± 0.3 ; $n=7$; 7.6 ± 0.2 ; $n=7$; TRAM-34 ($10 \mu M$): $69 \pm 4\%$; 8.0 ± 0.2 ; $n=13$; TRAM-34 ($10 \mu M$) and apamin ($1 \mu M$): $72 \pm 2\%$; 8.1 ± 0.2 ; $n=14$). L-NAME reduced E_{max} ($5 \pm 2\%$) and did not alter the pD_2 values (7.6 ± 0.2) when compared to acetylcholine relaxation in control tissues.

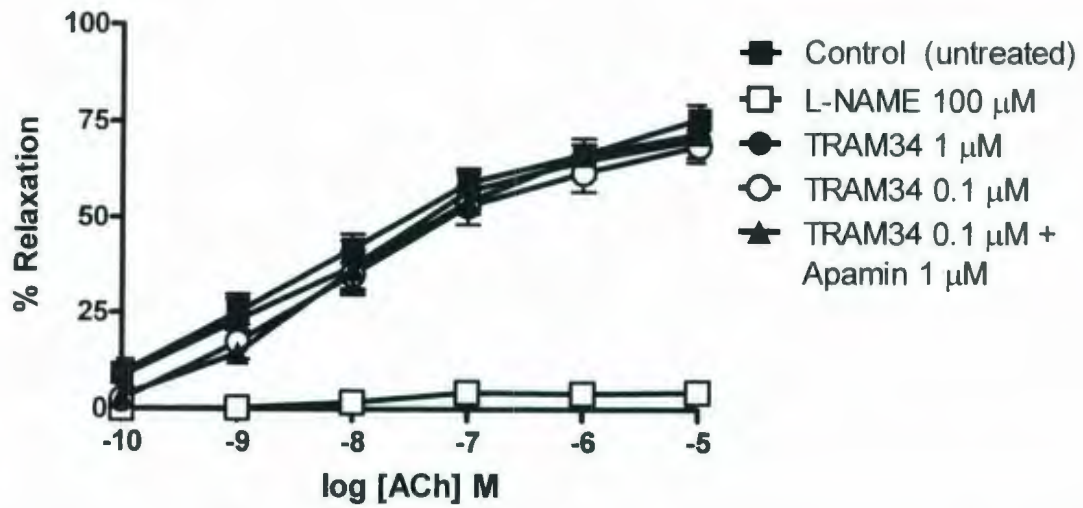


Figure 13 – Effects of L-NAME and K_{Ca} inhibitor on acetylcholine-induced relaxations of mouse aorta. Untreated (controls; n=15), L-NAME (n=7), TRAM-34 (IK_{Ca} inhibitor; 1 μ M n=7; 10 μ M n=13) or TRAM-34 + apamin (SK_{Ca} inhibitor; n=14)-treated aorta were contracted by U46619 (100 nM) prior to determining cumulative concentration response relaxation responses. Values are mean \pm sem.

SNP-induced relaxations of C57B6 aorta.

The relaxation responses of aorta to an endothelium-independent nitrovasodilator were tested with SNP (Figure 14). Potency and maximum responses did not differ between groups (E_{max} and pD_2 : Control: $87 \pm 2\%$; 8.9 ± 0.1 ; $n=15$; TRAM-34 (1 μM): $82 \pm 3\%$; 8.7 ± 0.2 ; $n=7$; L-NAME (100 μM): $87 \pm 2\%$; 8.9 ± 0.2 ; $n=7$; TRAM-34 (10 μM): $83 \pm 3\%$; 8.7 ± 0.2 ; $n=13$; TRAM-34 (10 μM) and apamin (1 μM): $83 \pm 2\%$; 8.8 ± 0.2 ; $n=14$) (Figure 14).

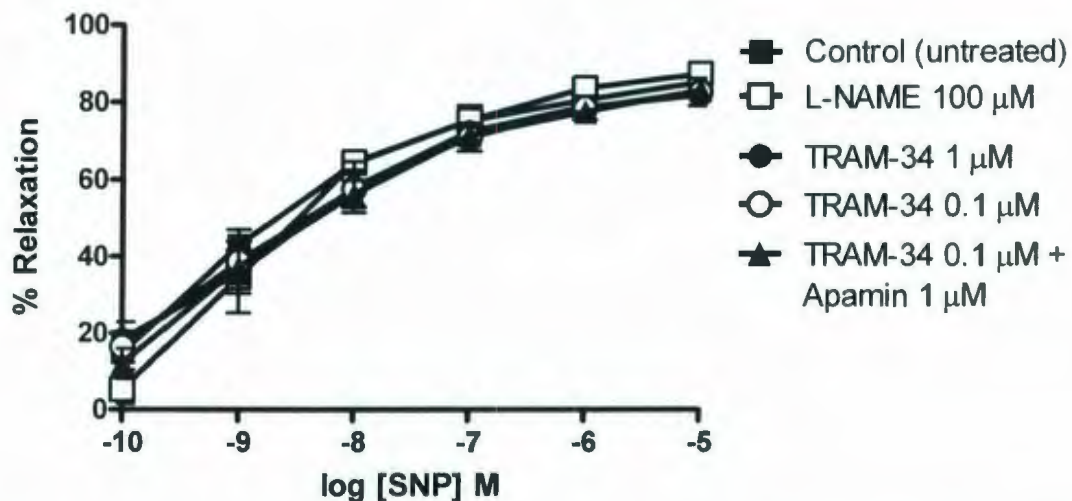


Figure 14 – Effect of inhibitor of K_{Ca} on SNP-induced relaxations of mouse aorta. Untreated (controls, $n=15$), L-NAME- ($n=7$), TRAM-34- (IK_{Ca} inhibitor; 1 μM , $n=7$; 10 μM , $n=13$) or TRAM-34 + apamin (SK_{Ca} inhibitor; $n=14$)-treated arteries were contracted by U46619 (100 nM) prior to determining relaxation responses to cumulative concentrations of SNP. Values are mean \pm sem.

Discussion

General findings

The first objective of this thesis was to determine if mMCP-7 activates PAR2 in the mouse aorta. We found that mMCP-7 did not relax mouse aorta even after deglycosylation of mouse aorta by neuraminidase. This occurred despite the confirmation that neuraminidase treatment enabled hMC β -tryptase-sensitive relaxations to occur in the mouse aorta. Since PAR2 activation was observed using the positive controls of PAR2-AP 2fly and PAR2 activating enzyme trypsin, we conclude that mMCP-7 did not activate PAR2 in mouse aorta at the amounts tested in this study. We believe these data indicate that the mMCP-7 isoform of mouse mast cell protease does not reproduce the full range of actions attributed to hMC β -tryptase. However, the experiments contained several limitations. The relative serine proteinase trypsin-like activity of the mMCP-7 that was employed in the relaxation assays was low. This warrants cautious interpretation of these data and possible further study using higher amounts of enzyme activity.

The second objective of this thesis was to determine if SK_{Ca} and IK_{Ca} inhibitors inhibit PAR2-mediated NO-dependent relaxation of mouse aorta. The mouse aorta is known to utilise NO for relaxation by PAR2 and it has been established that PAR2 activation activates K_{Ca} channels in smaller resistance arteries like mesenteric and middle cerebral arteries (McGuire et al., 2004; McGuire et al., 2007; Smeda and McGuire, 2007). Because there are no reports indicating the selective expression of K_{Ca} distribution amongst different endothelial cells, we hypothesised that if PAR2 activated K_{Ca} channels in aortic endothelium such action could enhance NO production and thus, the inhibitors of these channels should inhibit PAR2 relaxation of mouse aorta. We found that the

inhibitors of SK_{Ca} and IK_{Ca} either alone or in combination (using concentrations that would inhibit PAR2 in small arteries (McGuire *et al.*, 2004; McGuire *et al.*, 2007) did not inhibit PAR2-induced relaxation of mouse aorta. The K_{Ca} inhibitor treatments also did not inhibit endothelial-dependent relaxations by ACh or endothelium-independent relaxations by sodium nitroprusside. Treatment of aortas with the NO synthase inhibitor L-NAME blocked relaxations by both 2fly and ACh. Therefore, it appears that despite the ability of PAR2 to activate K_{Ca}, these channels plays no role in NO-mediated relaxations of contracted mouse aorta by PAR2-AP, ACh nor SNP.

Activation of PAR2 by serine proteinases in C57B6 aorta

Failure of mMCP-7 to produce any relaxation of contracted C57B6 aorta was an unexpected result so experiments were undertaken to compare these responses to other serine proteinases in the mouse aorta. Compton *et al.* (2002) demonstrated that hMCβ-tryptase was capable of activating PAR2 relaxation in rat aorta after deglycosylation of the tissue. While mMCP-7 was unable to elicit PAR2 relaxations, we did find that hMCβ-tryptase was capable of activating mouse PAR2 after neuraminidase treatment of tissues. This finding was consistent with the notion that in human tissues that hMCβ-tryptase is an endogenous activator of PAR2.

In C57B6 aorta, ACh and 2fly produced significant relaxation responses in controls and neuraminidase-treated tissues so the endothelium and PAR2 receptors were functionally intact in our experiments. Relaxations by 2fly and acetylcholine were not significantly different in neuraminidase-treated and control tissues, which also would support the notion that neuraminidase treatment did not alter the efficacy of endothelial PAR2 and muscarinic receptor mediated vasodilation. We demonstrated that 2fly elicited

relaxations were dependent on the expression of PAR2 since responses were absent in PAR2 ^{-/-} aorta. We used bovine pancreas trypsin, a known positive control for serine proteinase activation of PAR2, to demonstrate relaxation responses in C57B6 aorta. Trypsin had been chosen for a secondary purpose allowing us to standardise the amount of enzyme added to preparations relative to the units of trypsin activity. In our standardisation protocol experiments, BAPNA was used to as the substrate for peptide amidolytic activity. It seems possible that the differences between trypsin, hMCβ-tryptase and mMCP-7 with respect to causing vasodilation could be related to the low level of equivalent enzyme activity in respect to mMCP-7. This was due to a limitation in the amount of recombinant mMCP-7 which could be purchased and the amount of purified hMCβ-tryptase provided by collaborators. Further studies with enzyme preparations having higher specific activities and more direct assays of PAR2 activation are warranted.

In addition, the enzyme activities within the myograph chambers were less than optimal under the conditions of the bioassay. P20 peptide (³⁰GPNSKGR/SLIGRLDTP⁴⁵-YGCG) was incubated with mMCP-7 and mouse aorta to determine whether the enzyme could produce the PAR2 recognition sequence (SLIGRL). A similar approach had been used with hMCβ-tryptase and rat aorta (Compton *et al.*, 2002) which employed identical bioassay conditions. We found that mMCP-7 did not elicit relaxation in the presence of P20 so these experiments were repeated with tissues exposed to trypsin and hMCβ-tryptase. In C57B6 aorta, equivalent amounts of hMCβ-tryptase and trypsin were added to the tissue bath to match the activity of the mMCP-7 used previously. P20 elicited a relaxation from aorta only at the highest amount of trypsin. Surprisingly, P20 plus

equivalent (to trypsin) amounts of hMC β -tryptase did not produce any relaxation responses. We speculate that the rates of hydrolysis of soluble P20 and the *in situ* PAR2 tethered ligand differed with respect to the rates of activating PAR2. Alternatively PAR2 activation by hMC β -tryptase in mouse aorta may require a specific conformation of the tethered ligand that binds to PAR2 (like thrombin to PAR1) in order to achieve the subsequent activated receptor conformation. Finally, the negative findings could have indicated that mMCP-7 while recognising PAR2 as a substrate may have acted to disarm PAR2 rather than activate it. This possibility was not ruled-out by the experiments we performed. However, aortas did not show any tachyphylaxis to PAR2-AP after mMCP-7 treatment which would have indicated internalization following receptor disarming.

SK_{Ca} and IK_{Ca} interaction with NO-mediated relaxation in C57B6 aorta

In our study, the inhibition of NO synthases by L-NAME was sufficient to block 2fly and ACh-induced relaxations of C57B6 aorta, confirming the central role of NO in endothelium-dependent relaxation of this artery (McGuire *et al.*, 2002b; McGuire *et al.*, 2004). Since apamin and TRAM-34 did not affect either 2fly or ACh-induced relaxations, SK_{Ca} and IK_{Ca}, likely do not play a role in modulating endothelial NO-dependent relaxations. SNP relaxation responses were also unchanged in the presence of TRAM-34, apamin and L-NAME, suggesting that the pathways subsequent to NO generation were insensitive to SK_{Ca} and IK_{Ca} blockers. One interpretation of the data is that having PAR2 linked to SK_{Ca} and IK_{Ca} channels may be of no functional consequence in the endothelium of aorta.

The ineffectiveness of K_{Ca} inhibitors in altering endothelial-dependent relaxation responses in larger conductance sized artery like the aorta of C57B6 mice invites further

explanation. In small resistance arteries, PAR2 activation of K_{Ca} is considered to be essential to initiate an EDH response mediated by myoendothelial cell gap junctional communication between cells. This hyperpolarization results in dilation of the arteries. The inhibition of K_{Ca} also results in complete or partial inhibition of relaxation of other endothelial-dependent vasodilators such as acetylcholine and bradykinin in mouse mesenteric arteries and rat middle cerebral arteries (McGuire et al., 2007; Smeda and McGuire, 2007; Pannirselvam et al., 2006). We offer two explanations why an EDH response is unseen during PAR2-induced relaxation in C57B6 aorta. The first explanation is based on the assumption that PAR2 initiates a mechanism of action for vasodilation in all arterial beds in the same manner. That is, in small resistance arteries PAR2 activates NO synthase as well as an EDH response, which is well-supported by data (McGuire *et al.*, 2002; McGuire *et al.*, 2004; McGuire *et al.*, 2007). In comparison, in larger conductance arteries while PAR2 activates endothelial NO synthase it also initiates the endothelial K_{Ca} activation, but that the conduction of hyperpolarization is blocked by the physical composition of the aortic wall. That is, the internal lamina and elastin within internal layers of aortic wall may act as an electrical insulating barrier which would block any hyperpolarization response produced by PAR2 and similar EDH-initiating vasodilating agents except at sporadic gap junctions. Differential myoendothelial gap junction communication i.e. as a result of the internal elastic lamina or the specific isoforms of gap junction connexins present, may also explain the lack of an EDH response in mouse aorta. Such differences have been observed from high resolution electron microscopic morphological comparisons of rat femoral to rat mesenteric arteries (Sandow and Hill, 2000) and mRNA expression patterns in mice (Ceroni et al., 2007). An

alternative explanation is that receptors have adapted to signalling mechanisms that are also associated with the function of the different vascular beds. In smaller arterial beds where diameter changes are more responsible for regulating blood flow, PAR2 may have adapted to utilize a NO driven relaxation as well as an EDH response, which tends to be a more rapid response. In larger conduction arteries, PAR2 may only need to utilize NO, which functions physiologically less to control vascular tone, but to maintain an anti-thrombotic surface on the endothelium of large diameter arteries. If the latter argument holds merit then the link of PAR2 to K_{Ca} and the roles played by K_{Ca} may also be more important to other cellular functions of the endothelium in the aorta, for example, perhaps the release of cytokines in response to injury, which were not examined by this thesis.

Conclusions

mMCP-7 did not appear to activate PAR2 as bioassayed in C57B6 aorta at the amounts tested in this study. Given these findings mMCP-7 did not reproduce the actions of hMC β -tryptase on PAR2 on the endothelium and vascular smooth muscle of mouse aorta. We conclude that cautious interpretation of experiments is advised when investigating the roles played by mast cells and PAR2 in mouse models of cardiovascular diseases because enzymes target substrates may not be conserved across species.

Inhibitors of SK $_{Ca}$ and IK $_{Ca}$ did not inhibit the NO-dependent relaxation responses of ACh, SNP or 2fly in C57B6 aorta contracted by U46619. We conclude that K_{Ca} do not play any role in contributing to relaxation by PAR2 and NO release in "healthy" C57B6 aorta. We speculate that the link of PAR2 to K_{Ca} may contribute to endothelial cell function/dysfunction (other than by modulating vascular tone) in cardiovascular pathophysiology e.g. Ca²⁺-driven gene expression (Wang *et al.*, 2007).

References

al-Ani B, Saifeddine M, Hollenberg MD. Detection of functional receptors for the proteinase-activated-receptor-2-activating polypeptide, SLIGRL-NH₂, in rat vascular and gastric smooth muscle. *Can J Physiol Pharmacol.* (1995) **73**(8): 1203-1207.

Atkinson NS, Robertson GA, Ganetzky B. A component of calcium-activated potassium channels encoded by the *Drosophila slo* locus. *Science.* (1991) **253**(5019): 551-555.

Barbara G, Wany B, Stanghelli V, de Giorgio R, Cremon C, Di Nardo G, Trevisani M, Campi B, Geppetti P, Tonini M, Bunnett NW, Grundy D, Corinaldesi R. Mast cell-dependent excitation of visceral-nociceptive sensory neurons in irritable bowel syndrome. *Gastroenterology.* (2007): **132**(1): 26-37.

Berger P, Tunon-De-Lara JM, Savineau JP, Marthan R. Selected contribution: tryptase-induced PAR-2-mediated Ca²⁺ signaling in human airway smooth muscle cells. *J. Appl. Physiol.* (2001) **91**: 995-1003.

Bono F, Lamarche I, Herbert JM. Induction of vascular smooth muscle cell growth by selective activation of the proteinase activated receptor-2 (PAR-2). *Biochem Biophys Res Commun.* (1997) **241**: 762-764.

Cairns JA. Inhibitors of mast cell tryptase beta as therapeutics for the treatment of asthma and inflammatory disorders. *Pulmonary Pharmacol. & Therap.* (2005) **18**: 55-66.

Castells M, Irani AA, Schwartz LB. Evaluation of human peripheral blood leukocytes for mast cell tryptase. *J. Immunol.* (1987) **138**: 2184-2189.

Cenac N, Coelho AM, Nguyen C, Compton S, Andrade-Gordon P, MacNaughton WK, Wallace JL, Hollenberg MD, Bunnett NW, Garcia-Villar R, Bueno L, Vergnolle N. Induction of intestinal inflammation in mouse by activation of proteinase-activated receptor-2. *Am J Pathol.* (2002) **161**: 1903-1915.

Ceroni L, Ellis A, Wiehler WB, Jiang YF, Ding H, Triggle CR. Calcium-activated potassium channel and connexin expression in small mesenteric arteries from eNOS-deficient (eNOS^{-/-}) and eNOS-expressing (eNOS^{+/+}) mice. *Eur J Pharmacol.* (2007) **560**(2-3): 193-200.

Chung WO, Hansen SR, Rao D, Dale BA. Protease-activated receptor signaling increases epithelial antimicrobial peptide expression. *J. Immunol.* (2004) **173**: 5165-5170.

Coico R, Sunshine G, Benjamini E. *Immunology: a short course*. A John Wiley & Sons Inc.: Hoboken, New Jersey. 2003.

Cocks TM, Moffatt JD. Protease-activated receptors: sentries for inflammation? *Trends Pharmacol Sci.* (2000) **21**(3): 103-108.

Coleman HA, Tare M, Parkington HC. Endothelium potassium channels, endothelium dependent hyperpolarization and the regulation of vascular tone in health and disease. *Clinical and Exp. Pharmacol. Physiol.* (2004) **31**:641-649.

Coleman HA, Tare M, Parkington HC. EDHF is not K^+ but may be due to spread of current from endothelium in guinea pig arterioles. *Am. J. Physiol. Heart Circ. Physiol.* (2001) **280**: H2478-2483.

Compton, S.J., McGuire, J.J., Saifeddine, M., Hollenberg, M.D. Restricted ability of human mast cell tryptase to activate proteinase-activated receptor-2 in rat aorta. *Can. J. Physiol. Pharmacol.* (2002) **80**: 987-992.

Compton SJ, Sandhu S, Wijesuriya SJ, Hollenberg MD. Glycosylation of human proteinase-activated receptor 2: role in cell surface expression and signaling. *Biochem. J.* (2002) **368**:495-505.

Compton SJ, Renaux B, Wijesuriya SJ, Hollenberg MD. Glycosylation and the activation of proteinase-activated receptor 2 by human mast cell tryptase. *Br. J. Pharmacol.* (2001) **134**: 705-718.

Connolly AJ, Ishihara H, Kahn ML, Farese RV, Coughlin SR: Role of the thrombin receptor in development and evidence for a second receptor. *Nature.* (1996) **381**:516-519.

Cottrell GS, Amadesi S, Schmidlin F, Bunnett N. Protease-activated receptor 2: activation, signaling and function. *Biochem. Soc. Transactions* (2003) **31**(6):1191-1197

Coughlin SR, Camerer E. PARTicipation in inflammation. *J. Clin. Invest.* (2003) **278**(33): 30975-84.

Crane GJ, Gallagher N, Dora KA, Garland CJ. Small- and intermediate-conductance calcium-activated K^+ channels provide different facets of endothelium-dependent hyperpolarization in rat mesenteric artery. *J. Physiol.* (2003) **553**(1): 183-189.

D'Andrea MR, Derian CK, Leturcq D, Baker SM, Brunmark A, Ling P, Darrow AL, Santulli RJ, Brass LF, Andrade-Gordon P. Characterization of protease-activated receptor-2 immunoreactivity in normal human tissues. *The Journal of Histochemistry and Cytochemistry.* (1998) **46**: 157-164.

Damiano BP, D'Andrea MR, de Garavilla L, Cheung WM, Andrade-Gordon P. Increased expression of protease activated receptor-2 (PAR-2) in balloon-injured rat carotid artery. *Thromb Haemost.* (1999) **81**(5): 808-814.

De Campo BA, Henry PJ. Stimulation of protease-activated receptor-2 inhibits airway eosinophilia, hyperresponsiveness and bronchoconstriction in a murine model of allergic inflammation. *Br. J. Pharmacol.* (2005) **144**(8): 1100-1108.

Dery O, Corvera CU, Steinhoff M, Bunnett NW. Proteinase-activated receptors: novel mechanisms of signaling by serine proteases. *Am J Physiol.* (1998) **274**: C1429-C1452.

Edwards G, Thollon C, Gardener MJ. Role of gap junctions and EETs in endothelium-dependent hyperpolarization of porcine coronary artery. *Br. J. Pharmacol.* (2000) **129**: 1145-1154.

Edwards G, Félétou M, Gardener MJ, Thollon C, Vanhoutte PM, Weston AH. Role of gap junctions in the responses to EDHF in rat and guinea-pig small arteries. *Br. J. Pharmacol.* (1999) **128**:1788-1794.

Edwards G, Dora KA, Gardener MJ, Garland CJ, Weston AH. K^+ is an endothelium-derived hyperpolarization factor in rat arteries. *Nature* (1998) **396**: 269-272.

Fajardo I, Pejler G. Human Mast cell beta tryptase is a gelatinase. *J. Immunol.* (2003) **171**: 1493-1499.

Fanger CM, Ghanshani S, Logsdan NJ. Calmodulin mediates calcium-dependent activation of the intermediate conductance KCa channel, $IKCa1$. *J. Biol. Chem.* (1999) **274**(9):5746-5754.

Ferrell WR, Lockhart JC, Kelso EB, Dunning L, Plevin R, Meek SE, Smith AJ, Hunger GD, McLean JS, McGarry F, Ramage R, Jiang L, Kanke T, Kawagoe J. Essential role for proteinase-activated receptor-2 in arthritis. *J Clin Invest.* (2003) **111**(1): 35-41.

Fiorucci S, Mencarelli A, Palazzetti B, Distrutti E, Vergnolle N, Hollenberg MD, Wallace JL, Morelli A, Cirino G. Proteinase-activated receptor 2 is an anti-inflammatory signal for colonic lamina propria lymphocytes in a mouse model of colitis. *Proc. Natl. Acad. Sci. USA.* (2001) **98**(24): 13936-41.

Geppetti P, Trevisani M. Proteinase-Activated Receptors and Bronchial Smooth Muscle Functions. *Drug Development Research.* (2003) **60**: 24-28.

Gurish MF, Johnson KR, Webster MJ, Stevens RL, Nadeau JH. Location of the mouse mast cell protease 7 gene (*Mcpt7*) to chromosome 17. *Mammal. Genome* (1994) **5**:656-657

Gurish MF, Nadeau JH, Johnson KR, McNeil HP, Grattan KM, Austen KF, Stevens RL. A closely linked complex of mouse mast cell-specific chymase genes on chromosome 14. *J. Biol. Chem.* (1993) **268**:11372-11379.

Guyton AC, Hall JE. Textbook of Medical Physiology. *Elsevier Saunders* (2006)

Hamilton JR, Frauman AG, Cocks TM. Increased expression of protease-activated receptor-2 and PAR4 in human coronary artery by inflammatory stimuli unveils endothelium-dependent relaxations to PAR2 and PAR4 agonists. *Circ Res.* (2001) **136**: 492-501.

- Hamilton JR, Moffatt JD, Tatoulis J, Cocks TM. Enzymatic activation of endothelial proteinase-activated receptors is dependent on artery diameter in human and porcine isolated coronary arteries. *Br J Pharmacology*. (2002) **136 (4)**: 492-501.
- Hollenberg MD. Proteinase-mediated signaling: Proteinase-activated receptors (PARs) and much more. *Life Sciences*: (2003) **74**: 237-246.
- Holzhausen M, Spolidorio LC, Vergnolle N. Role of protease-activated receptor-2 in inflammation, and its possible implications as a putative mediator of periodontitis. *Mem. Inst. Oswaldo Cruz* (2005) **100**(suppl. I): 177-180.
- Howells GL, Macey MG, Chinni C, Hou L, Fox MT, Harriott P, Stone SR. Proteinase-activated receptor-2: expression by human neutrophils. *J. Cell. Sci.* (1997) **110**: 881-887.
- Huang C, Wong GW, Ghildyal N, Gurish MF, Sali A, Matsumoto R, Qiu WT, Stevens RL. The tryptase, mouse mast cell protease 7, exhibits anticoagulant activity *in vitro* and *in vivo* due to its ability to degrade fibrinogen in the presence of the diverse array of protease inhibitors in plasma. *J. Biol. Chem.* (1997) **272**(50):31885-31893.
- Hwa JJ, Ghibaudi L, Williams P, Chintala M, Zhang R, Chatterjee M, Sybertz E. Evidence for the presence of a proteinase-activated receptor distinct from the thrombin receptor in vascular endothelial cells. *Circ Res.* (1996) **78**(4): 581-588.
- Ishihara H, Connolly AJ, Zeng D, Kahn ML, Zheng YW, Timmons C, Tram T, Coughlin SR. Protease-activated receptor 3 is a second thrombin receptor in humans. *Nature* (1997) **386**: 502-506.
- Itoh T, Seki N, Suzuki S, Ito S, Kajikuri J, Kuriyama H. Membrane hyperpolarization inhibits agonist-induced synthesis of inositol 1,4,5-triphosphate in rabbit mesenteric arteries. *J. Physiol.* (1992) **451**:307-328.
- Jensen BS, Hertz M, Christophersen P, Madsen LS. The Ca²⁺-activated K⁺ channel of intermediate conductance: a possible target for immune suppression. *Expert Opin. Ther. Targets.* (2002) **6**(6):623-636.
- Jensen BS, Strobaek D, Christophersen P. Characterization of the cloned human intermediate-conductance Ca²⁺-activated K⁺ channel. *Am. J. Physiol.*. (1998) **275**:C848-C856.
- Kahn ML, Zheng YW, Huang W, Bigornia V, Zeng D, Moff S, Farese RV, Tam C, Coughlin SR. A dual thrombin receptor system for platelet activation. *Nature* (1998) **394**: 690-694.

Kamouchi M, Droogmans G, Nilius B. Membrane potential as a modulator of the free intracellular Ca²⁺ concentration in agonist-activated endothelial cells. *Gen Physiol Biophys.* (1999) **18**(2): 199-208.

Kawabata A, Kinoshita M, Kuroda R, Kakehi K. Capsazepine partially inhibits neurally mediated gastric mucus secretion following activation of protease-activated receptor 2. *Clin Exp Pharmacol Physiol.* (2002) **29**(4): 360-361.

Knaus HG, Eberhart A, Koch RO, Munujos P, Schmalhofer WA, Warmke JW, Kaczorowski GJ, Garcia ML. Characterization of tissue-expressed alpha subunits of the high conductance Ca(2+)-activated K⁺ channel. *J Biol Chem.* (1995) **270**(38): 22434-9.

Lerner DJ, Chen M, Tram T, Coughlin SR. Agonist recognition by proteinase-activated receptor 2 and thrombin receptor: importance of extracellular loop interactions for receptor function. *J. Biol. Chem.* (1996) **271**:13943-13947.

Lindner JR, Kahn ML, Coughlin SR, Sambrano GR, Schauble E, Bernstein D, Foy D, Hafezi-Moghadam A, Ley K. Delayed onset of inflammation in protease-activated receptor-2-deficient mice. *J. Immunol.* (2000) **165**: 6504-6510.

Lohn M, Jessner W, Furstanau M, Wellner M, Sorrentino V, Haller H, Luft FC, Gollasch M. regulation of calcium sparks and spontaneous transient outward currents by RyR3 in arterial vascular smooth muscle cells. *Circ Res.* (2001) **89**(11): 1051-1057.

Lourbakos A, Yuan YP, Jenkins AL, Travis J, Andrade-Gordon P, Santulli R, Potempa J, Pike RN. Activation of protease-activated receptors by gingipains from *Porphyromonas gingivalis* leads to platelet aggregation: a new trait in microbial pathogenicity. *Blood* (2001b) **97**: 3790-3797.

Maryanoff BE, Santulli RJ, McComsey DF, Hoekstra WJ, Hoey K, Smith CE, Addo M, Darrow AL, Andrade-Gordon P. Protease-activated receptor-2 (PAR-2): structure-function study of receptor activation by diverse peptides related to tethered-ligand epitopes. *Arch Biochem Biophys.* (2001) **386**(2): 195-204.

Maylie J, Bond CT, Herson PS, Lee WS, Adelman JP. Small conductance Ca²⁺-activated K⁺ channels and calmodulin. *J Physiol.* (2004) **554**(pt2):255-261.

McGuire JJ. Proteinase-Activated Receptor 2 (PAR2): A challenging New Target for Treatment of Vascular Diseases. *Current Pharmaceutical Design.* (2004) **10**: 2769-2778.

McGuire JJ, Dai J, Andrade-Gordon P, Triggle CR, Hollenberg MD. Proteinase-activated receptor-2 (PAR2): vascular effects of a PAR2-derived activating peptide via a receptor different than PAR2. *J Pharmacol Exp Ther.* (2002) **303**(3): 985-992.

- McGuire JJ, Ding H, Triggle CR. Endothelium-derived relaxing factors: a focus on endothelium-derived hyperpolarizing factor(s). *Can J Physiol Pharmacol.* (2001) **79(6)**: 443-70.
- McGuire JJ, Saifeddine M, Triggle CR, Sun K, Hollenberg MD. 2-Furoyl-LIGRLO-amide: A potent and selective proteinase-activated receptor 2 agonist. *Journal of Pharm. Exp. Thera.*(2004) **309**: 1124-1131.
- McGuire JJ, Hollenberg MD, Andrade-Gordon P, Triggle CR. Multiple mechanisms of vascular smooth muscle relaxation by the activation of Proteinase-Activated Receptor 2 in mouse mesenteric arterioles. *British Journal of Pharmacology*: (2002) **135**: 155-159.
- McGuire JJ, Hollenberg MD, Bennett BM, Triggle CR. Hyperpolarization of murine small caliber mesenteric arteries by activation of endothelial proteinase-activated receptor 2. *Can J Physiol Pharmacol.* (2004) **82(12)**: 1103-1112.
- McGuire JJ, Van Vliet BN, Gimenez J, King JC, Halfyard SJ. Persistence of PAR-2 vasodilation despite endothelial dysfunction in BPH/2 hypertensive mice. *Pflugers Arch.* (2007) **454(4)**: 535-543.
- McGuire JJ, Van Vliet BN, Halfyard SJ. Blood pressures, heart rate and locomotor activity during salt loading and angiotensin II infusion in protease-activated receptor-2 (PAR₂) knockout mice. *BMC Physiology* (2008) **8**:20.
- Molino M, Barnathan ES, Numerof R, Clark J, Dreyer M, Cumashi A, Hoxie JA, Schechter N, Woolkalis M, Brass LF. Interactions of mast cell tryptase with thrombin receptors and PAR-2. *J. Biol. Chem.* (1997) **272**: 4043-4049.
- Molino M, Raghunath PN, Kuo A, Ahuja M, Hoxie JA, Brass LF, Barnathan ES. Differential expression of functional protease activated receptor-2 (PAR-2) in human vascular smooth muscle cells. *Arterioscler Thromb Vasc Biol.* (1998) **18**: 825-832.
- Mulvany MJ, Halpern W. Contractile Properties of Small Arterial Resistance Vessels in Spontaneously Hypertensive and Normotensive Rats. *Circ. Res.* (1977) **41**:19-26.
- Napoli C, Pinto A, Cirino G. Pharmacological modulation, preclinical studies, and new clinical features of myocardial ischemic preconditioning. *Pharmacol Ther.* (2000) **88(3)**: 311-331.
- Nishikawa H, Kawabata A. Modulation of Gastric function by Proteinase-Activated Receptors. *Drug Development Research.* (2003) **60**: 9-13.
- Noorbakhsh F, Power C. Proteinase-Activated Receptor Expression and Function in the Brain. *Drug Development Research.* 2003 **60**: 51-57.

- Nystedt S., Ramakrishnan V., Sundelin J. The proteinase-activated receptor 2 is induced by inflammatory mediators in human endothelial cells. Comparison with the thrombin receptor. *J Biol Chem I.* (1996) **271** (25): 14910-15
- Okamoto T, Nishibori M, Sawada K, Iwagaki H, Nakaya N, Jikuhara A, Tanaka N, Saeki K. The effects of stimulating protease-activated receptor-1 and -2 in A172 human glioblastoma. *J. Neural Transm.* (2001) **108**: 125-140.
- Payne V, Kam PCA. Mast cell tryptase: a review of its physiology and clinical significance. *Anaesthesia.* (2004) **59**: 695-703.
- Pereira PJ, Bergner A, Ribeiro M, Huber R, Mastchiner G, Fritz H. Human beta tryptase is a ring-like tetramer with active sites facing a central pore. *Nature* (1998) **392**: 306-311.
- Randall D, Burggren W, French K. 2002. *Eckert Animal Physiology: mechanisms and adaptations.* W.H. Freeman and Company: New York, NY
- Sabri A, Gua J, Elouardighi H, Darrow AL, Anorade-Gordon P, Steinberg SF. Mechanisms of PAR4 actions in cardiomyocytes: Role of Src tyrosine kinase. *J. Biol. Chem.* (2003) **278**: 11714-11720.
- Saifeddine M, al-Ani B, Cheng CH, Wang L, Hollenberg MD. Rat proteinase-activated receptor-2 (PAR-2): cDNA sequence and activity of receptor-derived peptides in gastric and vascular tissue. *Br. J. Pharmacol.* (1996) **118**(3): 521-530.
- Sandow SL, Hill CE. Incidence of myoendothelial gap junctions in the proximal and distal mesenteric arteries of the rat is suggestive of a role in endothelium-derived hyperpolarizing factor-mediated responses. *Circ. Res.* (2000) **86**(3): 341-446.
- Schmidlin F, Amadesi A, Dabbagh K, Lewis DA, Knott P, Bunnett N. Proteinase-activated receptor 2 mediates eosinophil infiltration and hyper reactivity in allergic inflammation of the airway. *J. Immunol.* (2002) **169**: 5315-5321.
- Schmidlin F, Bunnett NW. Protease-activated receptors: how proteases signal to cells. *Curr. Opi. Pharmacol.* (2001) **1**:575-582.
- Schultheiss M, Neumcke B, Richter HP. Endogenous trypsin receptors in *Xenopus* oocytes: linkage to internal calcium stores. *Cell. Mol. Life Sci.* (1997) **53**: 842-849.
- Shpacovitch VM, Varga G, Strey A, Gunzer M, Buddenkotte J, Vergnolle N, Sommerhoff CP, Grabbe S, Gerke V, Homey B, Hollenberg M, Luger TA, Steinhoff M. Agonists of pteinase-activated receptor-2 modulate human neutrophil cytokine secretion, expression of cell adhesion molecules and migration within 3-D collagen lattices. *J. Leuko. Biol.* (2004) **76**: 388-398.

- Smeda JS, McGuire JJ. Effects of poststroke losartan versus captopril treatment on myogenic and endothelial function in the cerebrovasculature of SHRsp. *Stroke* (2007) **38**(5): 1590-1596.
- Sobey CG, Moffatt JD, Cocks TM. Evidence for selective effects of chronic hypertension on cerebral artery vasodilatation to protease-activated receptor-2 activation. *Stroke* (1999) **30**(9): 1933-1940.
- Steinhoff M, Buddenkotte J, Shpacovitch V, Rattenholl A, Moormann C, Vergnolle N, Luger TA, Hollenberg MD. Proteinase-activated receptors: transducers of proteinase-mediated signaling in inflammation and immune response. *Endocrine Reviews* (2005) **26**(1): 1-43.
- Thomas VA, Wheelless CJ, Stock MS, Johnson DA. Human mast cell tryptase fibrinogenolysis: Kinetics, anticoagulation mechanisms and cell adhesion disruption. *Biochemistry*. (1998) **38**: 2291-2298.
- Toro L, Wallner M, Meera P, Tanaka Y. Maxi K_{ca}: a unique member of the voltage-gated K channel superfamily. *News physiol. Sci.* 1998.
- Trejo J, Altschuler Y, Fu HW, Mostov KE, Coughlin SR. Protease-activated receptor-1 down-regulation: a mutant HeLa cell line suggests novel requirements for PAR1 phosphorylation and recruitment to clathrin-coated pits. *J. Biol. Chem.* (2000) **275**:31255-31265
- Triggle CR, Howarth A, Cheng ZJ, Ding H. Twenty-five years since the discovery of endothelium-derived relaxing factor (EDRF): does a dysfunctional endothelium contribute to the development of type 2 diabetes? *Can J Physiol Pharmacol.* (2005) **83**: 681-700.
- Vanhoutte PM. Endothelial dysfunction and vascular pathology. *Bull. Mem. Acad. R. Med. Belg.* (2006) **161**: 529-536.
- Vergara C, Latorre R, Marrion NV, Adelman JP. Calcium-activated potassium channels. *Curr. Opin. Neurobiol.* (1998) **8**:321-329.
- Vergnolle N, Bunnett NW, Sharkey KA, Brussee V, Compton SJ, Grady EF, Cirino G, Gerard N, Basbaum AI, Andrade-Gordon P, Hollenberg MD, Wallace JL. Proteinase-activated receptor 2 and hyperalgesia: A novel pain pathway. *Nat Med.* (2001) **7**(7): 821-826.
- Vergnolle N. Proteinase-activated receptor-2-activating peptides induce leukocyte rolling, adhesion, and extravasation in vivo. *J. Immunol.* (1999) **163**: 5064-5069.
- Vergnolle N, Macnaughton WK, Al-Ani B, Saifeddine M, Wallace JL, Hollenberg MD. Proteinase-activated receptor 2 (PAR2)-activating peptides: identification of a receptor

distinct from PAR2 that regulates intestinal transport. *Proc Natl Acad Sci U.S.A.* (1998) **95**(13): 7766-7771.

Vu T.K, Hung DT, Wheaton VI, Coughlin SR. Molecular cloning of a functional thrombin receptor reveals a novel proteolytic mechanism of receptor activation. *Cell.* (1991) **64**: 1057-1068.

Wang Y, Luo W, Reiser G. The role of calcium in protease-activated receptor-induced secretion of chemokine GRO/CINC-1 in rat brain astrocytes. *J Neurochem* (2007) **103**(2): 814-819.

Yan JC, Ma GS, Wu ZG, Kong XT, Zong RQ, Zhan LZ. Increased levels of CD40-CD40 ligand system in patients with essential hypertension. *Clin. Chim. Acta.* 2005; 355: 191–196

Yoshinari S, Fujita S, Masui R, Kuramitsu S, Yokobori S, Kita K, Watnabe Y. Functional reconstitution of an archeal splicing endonuclease invitro. *Nucleic Acids Symp Ser (Oxf).* (2005) **49**: 103-104

Appendix A

Table 3 – Flow chart for hypothesis 1.

	Chamber 1	Chamber 2	Chamber 3	Chamber 4
Treatment 1	120 mM KCl	120 mM KCl	120 mM KCl	120 mM KCl
Treatment 2	U46619 DRC (10^{-10} - 10^{-6} M)			
Treatment 3	Neuraminidase treatment (40 min)	Vehicle	Neuraminidase treatment (40 min)	Vehicle
Treatment 4	ACh (100 μ M)			
Treatment 5	mMCP-7 (10mU)	mMCP-7 (10mU)	2fly (1 μ M)	2fly (1 μ M)

Table 4 – Flow chart for hypothesis 2.

	Chamber 1	Chamber 2	Chamber 3	Chamber 4	Chamber 5	Chamber 6	Chamber 7	Chamber 8
Treatment 1	120 mM KCl	120 mM KCl	120 mM KCl	120 mM KCl	120 mM KCl	120 mM KCl	120 mM KCl	120 mM KCl
Treatment 2	U46619 DRC (10^{-10} - 10^{-6} M)	U46619 DRC (10^{-10} - 10^{-6} M)	U46619 DRC (10^{-10} - 10^{-6} M)	U46619 DRC (10^{-10} - 10^{-6} M)	U46619 DRC (10^{-10} - 10^{-6} M)			
Treatment 3	L-NAME (100 μ M)	TRAM-34 (1 μ M)	TRAM-34 (10 μ M)	TRAM-34 (10 μ M), Apamin (1 μ M)	Vehicle	Vehicle	Vehicle	Vehicle
Treatment 4	ACh DRC	ACh DRC	ACh DRC	ACh DRC	ACh DRC	ACh DRC	ACh DRC	ACh DRC
Treatment 5	SNP DRC	SNP DRC	SNP DRC	SNP DRC	SNP DRC	SNP DRC	SNP DRC	SNP DRC
Treatment 6	2fly DRC	2fly DRC	2fly DRC	2fly DRC	2fly DRC	2fly DRC	2fly DRC	2fly DRC

